European Journal of Taxonomy 852: 1–30
https://doi.org/10.5852/ejt.2022.852.2003
ISSN 2118-9773
www.europeanjournaloftaxonomy.eu
2022 · Kuttalam S. *et al.*

Research article

urn:lsid:zoobank.org:pub:D127C46E-9904-4FCC-BDD8-478BDB51EFCA

Phylogenetic and morphological analysis of *Gloydius himalayanus* (Serpentes, Viperidae, Crotalinae), with the description of a new species

Sourish KUTTALAM [1], Vishal SANTRA [2], John Benjamin OWENS [3], Melvin SELVAN [4], Nilanjan MUKHERJEE [5], Stuart GRAHAM [6], Anatoli TOGRIDOU [7], Omesh K. BHARTI [8], Jingsong SHI [9], Kartik SHANKER [10] & Anita MALHOTRA [11,*]

[1,3,6,11] Molecular Ecology and Evolution at Bangor, School of Natural Sciences, Bangor University, Environment Centre Wales, Bangor LL57 2UW, Wales, UK.
[1,2,5] Society for Nature Conservation, Research and Community Engagement (CONCERN), Nalikul, Hooghly, West Bengal 712407, India.
[1,2,3] Captive & Field Herpetology Ltd, 13 Hirfron, Llaingoch, Holyhead, Anglesey LL65 1YU, Wales, UK.
[4] Deceased 10 February 2022. Endangered Wildlife Trust, Kookal, Dindigul, Tamil Nadu 624103, India.
[7] 86 Greenslade Grove, Hednesford, Cannock, Staffordshire WS12 1QR, UK.
[8] State Institute of Health & Family Welfare, Shimla, Himachal Pradesh 171009, India.
[9] Institute of Vertebrate Paleontology and Paleoanthropology, Chinese Academy of Sciences, Beijing 100044, China.
[9] Institute of Zoology, Chinese Academy of Sciences, Beijing 610041, China.
[10] Centre for Ecological Sciences, Indian Institute of Science, Bangalore 560012, India.

[*] Corresponding author: a.malhotra@bangor.ac.uk
[1] Email: bsu8d2@bangor.ac.uk
[2] Email: vishal@concern.org.in
[3] Email: jhw19vln@bangor.ac.uk
[5] Email: mukherjee.nilanjan91@gmail.com
[6] Email: bspc12@bangor.ac.uk
[7] Email: anatolitogridou@yahoo.gr
[8] Email: bhartiomesh@yahoo.com
[9] Email: shijingsong@ivpp.ac.cn
[10] Email: kshanker@gmail.com

[1] urn:lsid:zoobank.org:author:6BB19D4B-2A50-483C-8B9E-480E647EB998
[2] urn:lsid:zoobank.org:author:2B20FFFE-265D-4BCF-BC26-0759BE2A525C
[3] urn:lsid:zoobank.org:author:2B52FB3F-A53C-4613-B3DE-1CA54043181D
[4] urn:lsid:zoobank.org:author:8DC30C4A-2C8E-4F3E-BB80-CAE0D3E96248
[5] urn:lsid:zoobank.org:author:E72CB092-4911-4128-8BBD-2A5209C5FBDD
[6] urn:lsid:zoobank.org:author:CD208E79-26BF-42F5-9E9C-63E630E44F73
[7] urn:lsid:zoobank.org:author:ABE176E7-BA22-4F07-B2E8-85CE36D12B25

[8] urn:lsid:zoobank.org:author:0754C82D-5976-4617-A0D7-8E9B23B4C079
[9] urn:lsid:zoobank.org:author:82B98F77-2E95-43B5-9B34-92BE8759EF2B
[10] urn:lsid:zoobank.org:author:09E192D6-CBC5-4BAC-8913-BE878997829C
[11] urn:lsid:zoobank.org:author:C7B14F40-45CC-4A17-96FD-45C1031CD989

Abstract. *Gloydius* is a widespread pitviper group occurring from Eastern Europe to Korea and Siberia, with only one known species, *G. himalayanus* (Günther, 1864), found south of the Himalayas. We provide combined genetic and morphological data for *G. himalayanus* from specimens collected from Himachal Pradesh, India. Bayesian Inference and Maximum Likelihood phylogenetic analysis were performed on four concatenated mitochondrial genes, along with a multi-locus coalescent analysis of these and five additional nuclear genes. Our results indicate that *G. himalayanus* from the Chamba Valley, in western Himachal Pradesh, are highly distinct from the remaining studied populations. Haplotype networks of each nuclear locus showed that *G. himalayanus* contains high haplotype diversity with low haplotype sharing between the Chamba Valley population and populations from further west. Principal component analysis and canonical variate analysis conducted on morphological data of live and museum specimens also highlight the morphological distinctiveness of the Chamba population and we herein describe this population as a new species, *Gloydius chambensis* sp. nov. Recent descriptions of other new species of snakes from this valley underscores its isolation and suggests that further herpetological investigation of the highly dissected landscapes of the western Himalayas is needed to assess the true diversity of the region.

Keywords. Western Himalayas, pitviper, multi-locus coalescent, Bayesian phylogenetics, multivariate morphometrics.

Kuttalam S., Santra V., Owens J.B., Selvan M., Mukherjee N., Graham S., Togridou A., Bharti O.K., Shi J., Shanker K. & Malhotra A. 2022. Phylogenetic and morphological analysis of *Gloydius himalayanus* (Serpentes, Viperidae, Crotalinae), with the description of a new species. *European Journal of Taxonomy* 852: 1–30. https://doi.org/10.5852/ejt.2022.852.2003

Introduction

The Asian pitviper, *Gloydius* Hoge & Romano-Hoge, 1981, is a genus of small-bodied venomous snakes that is distributed from far-eastern Russia, through central and northern Asia, and as far west as Azerbaijan. Formerly considered part of the *Agkistrodon* Palisot de Beauvois, 1799 complex, it is now recognised to be phylogenetically part of the Asian pitviper radiation (Malhotra *et al.* 2010; Alencar *et al.* 2016). Although the systematics of this group have been unclear in the past, and are yet to be fully resolved, 22 species are currently recognised in the genus and are categorised into three subgroups: the *G. blomhoffii* complex, the *G. intermedius–halys* complex, and the *G. strauchi* complex (Orlov & Barabanov 2000; Xu *et al.* 2012; Wagner *et al.* 2016; Shi *et al.* 2017, 2018).

Gloydius himalayanus (Günther, 1864) is the only species in the genus that is found on the southern slopes of the Himalayan range. Recently, the first mitochondrial phylogeny of *Gloydius* to include *G. himalayanus* showed that it is sister to, and highly divergent from, all other species of *Gloydius* (Shi *et al.* 2021). Holding the record for the highest-occurring snake species, at 4877 m (Wall 1910), *Gloydius himalayanus* is recorded across the Himalayas of northern Pakistan, northern India (Kashmir, Himachal Pradesh, Uttarakhand, Sikkim, and West Bengal), Nepal and Bhutan (Whitaker & Captain 2004; Chettri *et al.* 2011; Koirala *et al.* 2016; Chaudhuri *et al.* 2018). Records from the Khasi Hills appear to be erroneous (Gloyd & Conant 1990). They are found mainly in and around coniferous forests, where they take refuge under fallen leaves, fallen logs, crevices of rocks and under boulders (Khan & Tasnim 1986). They are also found in agricultural fields in parts of the distribution that overlap with human settlements (Whitaker & Captain 2004; Manhas 2020). There has been no recent work on intra-

specific variation in *G. himalayanus* since Gloyd and Conant reviewed the *Agkistrodon* complex in 1990. In their review, they noted considerable variation in coloration and patterning across individuals (Gloyd & Conant 1990). Variation was also noted by Khan & Tasnim (1986), where they stated that "A study of *Agkistrodon himalayanus*, throughout its range, may reveal a polymorphic nature".

In this study, we utilised four mitochondrial and five nuclear genes in a multi-locus coalescent analysis to investigate intra-specific variation in *G. himalayanus.* A deep genetic split, comparable to or exceeding that between established species, was found between populations sampled in different regions of Himachal Pradesh, India. This was further investigated using a multivariate morphometric approach. Despite a limited sample size, morphological analysis supported the distinct population as a novel species, and a description of this new species is provided.

Material and methods

Sample collection

Sample collection was undertaken in Himachal Pradesh, India, between 2017 and 2019 during July to September (monsoon season). Specimens were collected in Chamba, Kangra, Kullu, and Shimla districts (Fig. 1). Tissue samples were collected in the form of blood (max. 0.02 ml) from the caudal vein, as well as 3–5 scale clippings (ventral scales). Blood samples were added to 1 ml 5% EDTA and preserved in 1 to 5 ml SDS-Tris buffer (100 mM Tris, 3% SDS) and scale clippings were preserved in 95% ethanol. In the case of fresh roadkill specimens, liver tissue was collected and stored in 95% ethanol. All collected samples were transferred to the Centre for Ecological Sciences, Indian Institute of Science, Bangalore, India, for long-term storage, DNA extraction and further sequencing work.

DNA extraction and PCR amplification

DNA extractions were performed using the Qiagen DNeasy® Blood and Tissue Kit following the manufacturer's protocol (Qiagen 2020). Gel electrophoresis and a Nanodrop Spectrophotometer ND1000 were used for checking the concentration and quality of extracts.

Four mitochondrial genes, cytochrome b (Cytb), NADH dehydrogenase subunit four (ND4), 12S small subunit ribosomal RNA (12S), and 16S large subunit ribosomal RNA (16S) and five nuclear genes, oocyte maturation factor (cmos), prolactin receptor gene (PRLR), ubinuclein 1 (UBN1), recombination activating gene 1 (RAG1), and neurotrophin 3 (NT3) were PCR-amplified using Thermo Fisher Scientific DreamTaq Mastermix. The primers and reaction conditions used for each gene can be found in the Supp. file 1: Tables S1–S2. Successful amplification was confirmed using gel electrophoresis and PCR products were cleaned for sequencing using Thermofisher ExoSAP-IT and Sanger-sequenced at Bioscience Barcode (Bangalore, India).

Alignment and phasing

Resulting chromatograms were edited in MEGA7 (Kumar *et al.* 2016) to correct any errors, trim the ends, and detect heterozygous positions present in the nuclear gene sequences. Sites were assigned as heterozygotes if they were found in both forward and reverse sequences and were assigned the appropriate IUPAC ambiguity code. Each gene alignment was initially produced using MUSCLE (Edgar 2004) via MEGA7, with further manual adjustments to ensure that identical sequences had been aligned identically. Protein-coding genes were checked for unexpected stop codons, and chromatograms were reviewed, if these were found. Haplotypes were reconstructed using PHASE in DnaSP ver. 6 (Rozas *et al.* 2017). Since the sections of the genes used are relatively short, PHASE was set to assume no recombination.

Phylogenetic analysis of mitochondrial genes

MrBayes ver. 3.2.7 (Ronquist *et al.* 2012) was used to conduct Bayesian Inference (BI) analysis on the mitochondrial dataset. Additional species of *Gloydius* from all three species complexes (see above) and species of other Asian pitviper genera, *Protobothrops* Hoge & Romano-Hoge, 1983, *Ovophis* Hoge & Romano-Hoge, 1981, *Trimeresurus* Lacépède, 1804, *Viridovipera* Malhotra & Thorpe, 2004, and *Tropidolaemus* Wagler, 1830, as well as New World pitvipers, were also included, and the viperine *Bitis gabonica* (Duméril, Bibron & Duméril, 1854) was set as the outgroup. PartitionFinder ver. 2.1.1 (Lanfear *et al.* 2017) was used to determine the best-fit partition scheme for the alignment and the best-fit models of evolution for the partitioned subsets based on the Bayesian Information Criterion (BIC) scores. Four independent chains were run simultaneously for 10 000 000 generations with a sampling frequency of 5000. Convergence of likelihood and the appropriate cut-off to account for burn-in was ascertained using Tracer ver. 1.7.1, and the R-Studio (R Core Team 2020) package R We There Yet (RWTY) (Warren *et al.* 2017) was used to diagnose issues with topological convergence and mixing of MCMC chains.

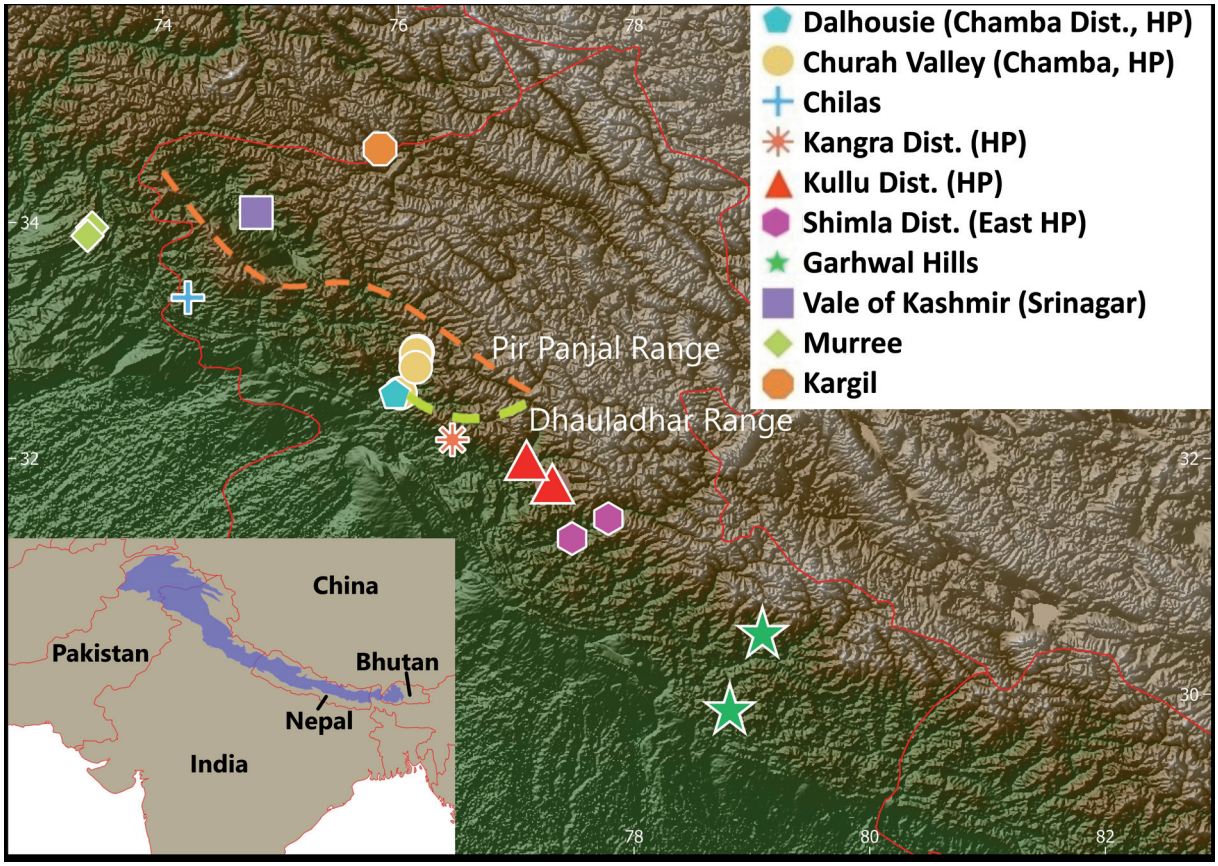

Fig. 1. Locations of all specimens used in the study for morphological and phylogenetic analysis. The position of two significant mountain ranges of the Lesser Himalayas, Pir Panjal and Dhauladhar, are indicated by dashed lines. An inset showing the current known distribution of *Gloydius himalayanus* (Günther, 1864) is also shown, with limits determined by the known altitudinal range (900–5000 m). The maps were constructed using Digital Elevation Models on QGIS ver. 3.22.1. The boundaries used on this map do not imply the expression of any opinion whatsoever on the part of the authors concerning the legal status of any country, territory, or area or of its authorities, or concerning the delimitation of its frontiers or boundaries. Dotted and dashed lines on maps represent approximate border lines for which there may not be full agreement.

A Maximum Likelihood tree was constructed using IQ-Tree (Nguyen *et al.* 2015) on the same dataset, using the partitioning scheme selected by PartitionFinder but with models selected under the Bayesian Information Criterion (BIC) by ModelFinder (Kalyaanamoorthy *et al.* 2017), which is implemented by IQ-Tree, with 10 000 UltraFast Bootstraps (UFB) (Minh *et al.* 2013).

Multi-locus coalescent phylogenetic analysis

The freeware program, *BEAST, implemented in the phylogenetic analysis package BEAST2 (Heled & Drummond 2010), was used to produce a multispecies coalescent phylogeny using all nine genes. Individual specimens were grouped into species in the taxa selection option. The mitochondrial gene trees were linked, and all other trees, evolutionary models and clock models were left unlinked.

To identify each evolutionary model, JModelTest ver. 2.1.1 was used (Guindon & Gascuel 2003; Darriba *et al.* 2012). The Standard Nucleotide Substitution Models ver. 1.0.1 package was also installed to allow the selection of the most appropriate models by JModelTest ver. 2.1.1 (Bouckaert & Xie 2017). Other settings were arrived at by comparing runs with different settings (e.g., "Relaxed Clock Log Normal" vs "Strict Clock") in a Bayes Factor test to compare marginal likelihoods of each run. Marginal likelihoods were estimated via path-sampling (Lartillot & Philippe 2004), with a chain length of 10 000 000 and 100 steps. The "Linear with constant root function" was selected, since there is a lack of information about population change at the root (Barido-Sottani *et al.* 2018). The ploidy for all nuclear gene trees was set to autosomal nuclear and the mitochondrial gene tree was set to Y or mitochondrial (Barido-Sottani *et al.* 2018). The population mean prior was changed from the default value of 1/X to log normal, and the clock rate for each gene was set to exponential (Heath 2015). The chain length was set to 1 000 000 000 with a sampling frequency of 100 000. The resulting .xml file was run three times with three different seeds and the trace log files were analysed using Tracer ver. 1.7.1 as above. The three species tree files were combined on LogCombiner with the appropriate burnin value, and the resulting species tree file was summarised using TreeAnnotator with default values (Barido-Sottani *et al.* 2018).

Nuclear haplotype networks

Haplotype networks were created for all nuclear loci, as the lower level of variation in these datasets suggests that ancestral haplotypes may still be present in the population, thus violating some of the assumptions of a phylogenetic approach (Bandelt *et al.* 1999) and allowing mutational steps between haplotypes to be reconstructed. Only sequences of species of *Gloydius* were included when creating the median-joining networks for each gene. The networks were created and visualised using Network ver. 10.2.0.0 (Fluxus Technology Ltd. – www.fluxus-engineering.com).

Population genetic metrics

Haplotype branch network diversity (HBd) was calculated in order to compare different clades for the nuclear gene networks. HBd estimates the complexity of haplotype networks by combining Hd and Bd to provide a probabilistic value that encompasses both the genetic diversity in a population as well as accounting for the topology diversity of networks (Garcia *et al.* 2021). The metrics were calculated in R-Studio following the guidelines provided by Garcia *et al.* (2021).

Morphological analysis

Live specimens obtained in the field were restrained using clear restraining tubes and the following data was measured wherever possible. In addition to data collected from specimens found in the field, museum specimens were also examined. Unfortunately, planned visits to museums with significant holdings such as the Natural History Museum (London, UK) and the Bombay Natural History Society (Mumbai, India) could not take place or had to be curtailed due to the restrictions in place as a result of the SARS-Cov-2 pandemic. For all specimens, with the exception of some very small juvenile specimens, sex was

recorded. Thirty-two specimens were examined in total, ranging from Eastern Pakistan to Uttarakhand (details are given in Appendix 1). The following characters were measured. Characters in bold type were found to be invariable in all specimens examined and not analysed further.

Abbreviations

Scale counts

3lab, 4lab, 5lab	=	number of scales between 3/4/5 upper labial and the lower postocular scale
Btwf	=	number of scales between the frontal scales
Btwpf	=	number of scales between the prefrontal scales
Chin	=	number of chin shields and median gulars (scales next to Lat gular)
Eye	=	number of scales between the preocular scale and the thermal pit
Fusedup	=	number of supralabial scales fused with the lower temporal scales
Intnas	=	shape of the border of the internasal scale and the prefrontal scale (0: flat or concave; 0.5: intermediate condition; 1: curved or convex)
LatGular	=	Number of gular scales in contact with the infralabial scales, excluding the enlarged chin shield
Midbody	=	number of scale rows at midbody
Nas	=	number of scales between pit and nasal scale
Postoc	=	number of postocular scales
SCS	=	Sub-Caudal Scale Count
Sublab	=	number of infralabial scales (average of both sides)
Suplab	=	number of supralabial scales (average of both sides)
Supoc	=	shape of the supraocular scale (0: completely smooth outer edge; 1: possessing a very defined notch in the outer edge)
Vent	=	number of scale rows immediately before the vent
VSC	=	Ventral Scale Count

Linear measurements (all in mm, measured at the widest point, unless otherwise stated)

Deye	=	diameter of the eye
FrontL	=	length of the frontal scale
FrontW	=	width of the frontal scale
Lhead	=	length of the head measured from the tip of the snout to the rear angle of the lower jaw
Lsupoc	=	length of supraocular
Rostl	=	length of rostral scale measured from top to bottom
Rostw	=	width of rostral scale measured from left to right
SVL	=	length from the tip of snout to vent (in cm) along the spine
Tail	=	length from the rear edge of the vent to the tip of the tail (in cm)
Whead1	=	width of head measured from the edges of the jaws
Wintnas	=	width of internasal
Wsupoc	=	width of the supraocular

Coloration (where bilateral, the longest feature was recorded)

Crossb	=	total number of cross bands after the neck stripe (crossband defined as a pair of bands with a dark inner edge and light-coloured outer edge)
Ocstripe	=	number of upper labial scales covered by the ocular stripe
Scoc	=	ventral scale position at which the ocular stripe ends
Spot25, spot50, spot 75, spot100	=	number of blotches/spots of darker coloration at 25%, 50%, 75% and 100% of the snout-vent length (a crossband can also be counted as a blotch/spot)

Stripe	=	ventral scale position of the end of the dark line on the neck
Strtemp	=	proportion of first temporal scale covered by the ocular stripe (0: no stripe on the scale; 1: stripe completely covers the scale)

Scale reduction formulae: for each scale reduction (from 25 to 17 scales on the body and from 14 to 5 scales on the tail) VS or SC position, where VS/SC was the average of the two ventral or subcaudal scales at which the scale reductions occur on either side, and DV, the average dorso-ventral position of the lowest of the two-scale rows involved in the scale reduction, were recorded.

All characters which depended on ventral or subcaudal scale counts (i.e., scale reductions and some colour pattern characters) were first converted to a percentage to account for variation in ventral or subcaudal scale counts. There were substantial amounts of missing data, with very few specimens having the full set of characters recorded. This was due to a combination of factors, including the difficulties of measuring some characters in live animals, time constraints during fieldwork, damage to road-killed specimens, and poor state of preservation and/or small size of museum specimens.

Because some grouping of specimens is necessary for preliminary processing (e.g., filling in missing values, eliminating uninformative characters), initial grouping was done conservatively and available specimens were grouped into the following locations (listed from west to east): Murree, East Pakistan (n = 2), Vale of Kashmir (n = 3), Kargil, Kashmir (n = 1), Chilas, Kashmir (n = 1), Churah, Chamba District, Himachal Pradesh (n = 7), Dalhousie, Chamba District, Himachal Pradesh (n = 5), Kullu Valley, Himachal Pradesh (n = 5), Eastern Himachal Pradesh (Great Himalayan National Park, Kullu District, and locations in Shimla districts) (n = 4), Garhwal, Uttarakhand (n = 2). Two museum specimens with vague locations (Kashmir, Himalayas) were left ungrouped at this stage and were not used for preliminary data analysis.

ANOVA was conducted on all non-mensural data using groups which had sufficient sample size ($n \geq 2$), along with a Levene's test (Levene 1961) to test the assumption of homoscedascity. If the latter was found to be violated, an alternative test which relaxes this assumption, the Brown-Forsythe (BF) test (Brown & Forsythe 1974), was used instead. For mensural data, an ANCOVA was carried out, using an appropriately correlated measure of size as the covariate. For most head measurements, this was Lhead, but for Lhead and Tail, SVL was used as covariate.

In all tests of variance, we first used sex as the factor to determine whether characters were sexually dimorphic, and subsequently used locality as the factor (with sexually dimorphic characters tested separately in males and females) to determine whether characters showed geographic variation. Only characters showing significant among-location variation were used in further analyses.

The next step was an unsupervised clustering method, principal component analysis (PCA). This does not require pre-grouping of specimens and is therefore the most suitable for exploratory analyses of morphological variation where the presence of more than one species is suspected and where the appropriate groups for specimens are not initially obvious. For mensural characters, the unstandardised residuals from the regression against the appropriate covariate were used, while meristic characters were first standardized (i.e., with zero mean, unit standard deviation). Qualitative characters were left untransformed. A Scree plot was examined to determine the number of axes to retain. Several different analyses were carried out to compensate for missing data, either maximising the number of characters (and reducing the number of specimens included) or maximising the inclusion of specimens (with a reduced number of characters). Once appropriate groups had been determined based on this analysis, missing data for non-mensural characters for a given group was replaced with the mean of the remaining specimens in that group if less than 30% of the data were missing for that group. If affinities were unclear, specimens were left ungrouped. A canonical variate analysis was then performed

on untransformed characters, using the pooled within-group covariance matrix for extraction and with ungrouped specimens included (thus they are not included in the canonical analysis but are plotted on the resulting canonical variates). Finally, a discriminant analysis was conducted between groups defined by the CVA in order to find reliable diagnostic characters.

All analyses were conducted in SPSS ver. 27 (SPSS Inc Chicago, US).

Results

Mitochondrial DNA analysis

The final dataset constituted 94 sequences with four mitochondrial genes totalling 2488 base pairs (12S: 423 bp, 16S: 491 bp, Cytb: 942, ND4: 632). All novel sequences were submitted to GenBank and are available under the accession numbers (OP407963-76; OP422579-629; OP450854-942; OP480160-7; OP508264-75; OP518267-80; OP776641); details are available in Supp. file 1: Table 3. PartitionFinder identified the best scheme to contain three subsets: subset1 consisted of 12S, 16S, the first codon position of Cytb and ND4 with the best model corresponding to GTR+I+G (Tavaré 1986); subset2 consisted of the second codon position of Cytb and ND4 with the best model corresponding to K81UF+I+G (Kimura 1981); and subset3 consisted of the third codon position of Cytb and ND4 with the best model corresponding to TIM+G (Posada 2003).

The output of the MrBayes analysis was analysed using the RWTY package on R-Studio and the graphs. The graphs produced indicated satisfactory mixing (Supp. file 1: Figs S1–S7). A Bayesian Inference (BI) tree was created using FigTree ver. 1.4.4 (Fig. 2). The mitochondrial tree was used to identify various clades of the *Gloydius* genus used as a reference in subsequent analyses.

Both the BI tree and ML tree also reiterate the finding reported in Shi *et al.* (2021) that *G. himalayanus* forms a basal lineage that is highly distinct from all other *Gloydius* species found north of the Greater Himalayan range. The trees also showed clear support for specimens from the Churah Valley in the east of Himachal Pradesh as a distinct group, with the rest of the samples forming a second clade (PP = 1.0, UFB = 100%).

Multi-locus species analysis

The dataset consisted of 133 sequences, assigned to 50 OTUs. The specimens of *G. himalayanus* sequenced in this study were assigned to a taxon labelled "Gloydius_himalayanus_HP1" for the Chamba specimens and the rest of the specimens were given the taxon label "Gloydius_himalayanus_HP2". The dataset contained all nine genes (12S: 423 bp, 16S: 491 bp, Cytb: 942 bp, ND4: 632 bp, cmos: 519 bp, NT3: 562 bp, PRLR: 298 bp, RAG1: 912 bp, UBN1: 467 bp). The evolutionary models for the different genes were set as follows: 12S: TIM2+G (Posada 2003); 16S: TIMef+I+G (Posada, 2003); Cytb: TIM3+I+G (Posada 2003); ND4: TrN+I+G (Tamura and Nei 1993); cmos: TPM3uf+I (Kimura 1981); NT3: K80+G (Kimura 1980); PRLR and RAG1: HKY+G (Hasegawa *et al.* 1985); UBN1: TIM1+G (Posada 2003). The path sampling analysis supported the "Strict Clock"(Δ BF= 179.539) and the "Birth-Death" (Δ BF= 179.539) priors.

The BI tree produced from this analysis is visualised in Figure 3. The two distinct clades present in *G. himalayanus* are also strongly supported (PP = 1.0). The basal and relatively distant position of *G. himalayanus* in relation to other species of *Gloydius* seen in the mitochondrial phylogenies was also strongly supported in the multi-locus analysis (PP = 0.99). All other clades within *Gloydius* seen in the mitochondrial analyses are also recovered in the multilocus analysis; however, these were unresolved with respect to each other in the mitochondrial analysis. In the multi-locus analysis, Clades C (*G. qinlingensis* Song & Chen, 1985) and D (*G. liupanensis* Liu, Song & Luo, 1989) form a single clade

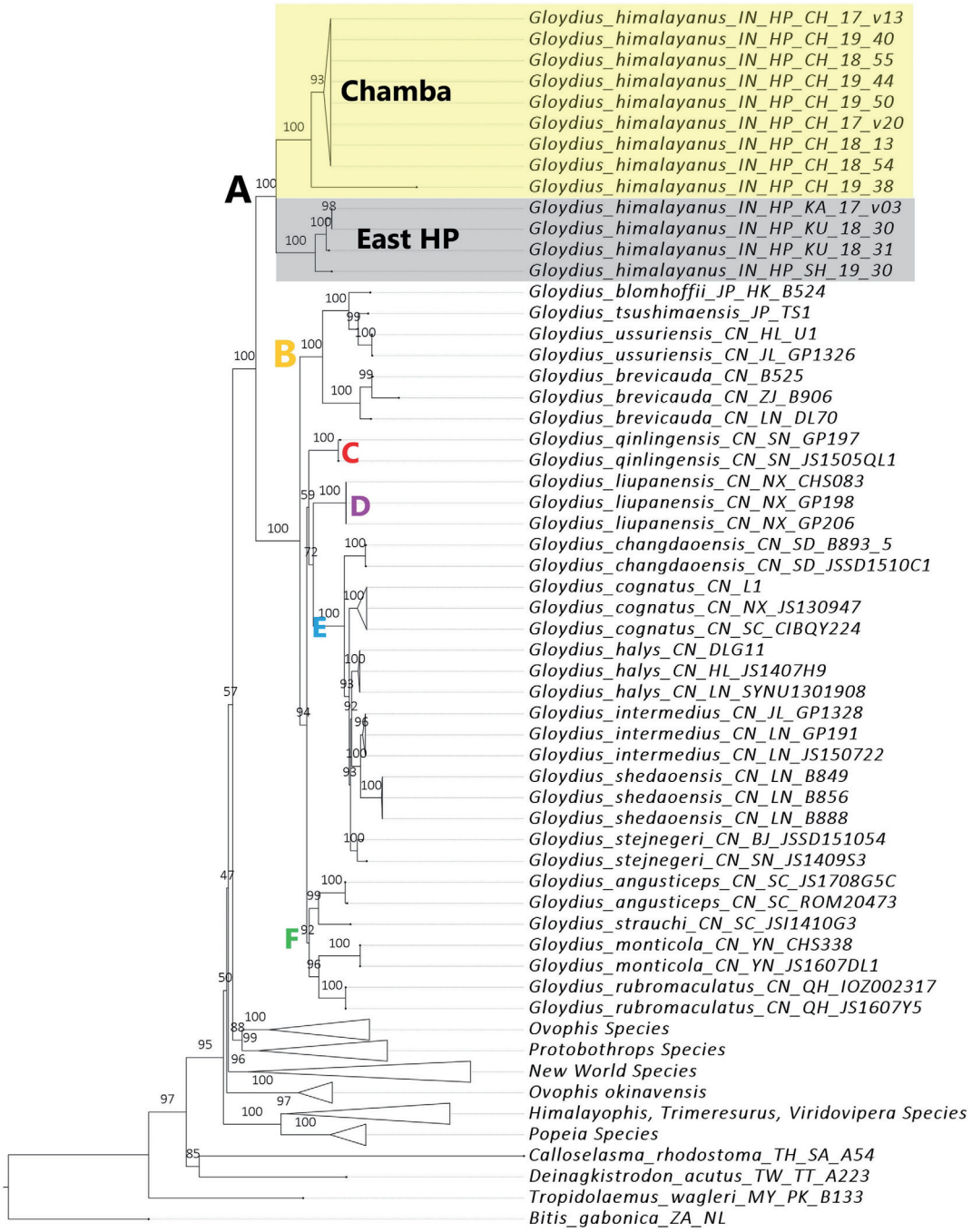

Fig. 2. Maximum-likelihood tree: branch labels indicate the ultrafast bootstrap support (%). In this and subsequent figures, each clade is labelled and designated in a particular colour. These clades correspond to: **A**. *Gloydius himalayanus* (Günther, 1864) (black). **B**. *G. blomhoffii* (H. Boie, 1826), *G. brevicauda* (H. Boie, 1826), *G. ussuriensis* (Emelianov, 1929) (yellow). **C**. *G. qinlingensis* Song & Chen, 1985 (red). **D**. *G. liupanensis* Liu, Song & Luo, 1989 (purple). **E**. *G. halys* (Pallas, 1776), *G. intermedius* (Strauch, 1868), *G. changdaoensis* Li, 1999, *G. cognatus* (Gloyd, 1977), *G. stejnegeri* (Rendahl, 1933), *G. shedaoensis* (Zhao, 1979) (blue). **F**. *G. angusticeps* Shi, Yang, Huang, Orlov & Li, 2018, *G. strauchi* (Bedriaga, 1912), *G. monticola* (F. Werner, 1922), *G. rubromaculatus* Shi, Wang, Chen, Fang, Ding, Huang, Hou, Liu & Li, 2017 (green).

(PP = 0.93), which is the sister group to Clade E (*G. halys* (Pallas, 1776), *G. intermedius* (Strauch, 1868), *G. cognatus* (Gloyd, 1977), *G. stejnegeri* (Rendahl, 1933), *G. shedaoensis* (Zhao, 1979)). *Gloydius changdaoensis* Li, 1999 was found to be the sister group to Clades C, D and E (PP = 1.00). These in turn are sisters to Clade F (*G. angusticeps* Shi, Yang, Huang, Orlov & Li, 2018, *G. strauchi* (Bedriaga, 1912), *G. monticola* (F. Werner, 1922), *G. rubromaculatus* Shi, Wang, Chen, Fang, Ding, Huang, Hou, Liu & Li, 2017) and Clade B (*G. blomhoffii* (Stejneger, 1907), *G. tsushimaensis* (Isogawa, Moriya & Mitsui, 1994), *G. ussuriensis* (Emelianov, 1929), *G. brevicauda* (H. Boie, 1826)) forms the sister group to all of these (Fig. 3).

Nuclear haplotype networks

All nuclear loci, apart from RAG1, showed *G. himalayanus* to contain genetically distant haplotypes from the rest of the genus (Fig. 4). In RAG1 (Fig. 4a), one haplotype from specimen 17.v13 of *G. himalayanus* was closer to haplotypes of *G. brevicauda*, and a haplotype of *G. blomhoffii* was closer to the rest of the haplotypes of *G. himalayanus*. Specimens of *Gloydius himalayanus* from Kullu Valley do not share any haplotypes with the Chamba specimens in the two loci in which both were represented, cmos and PRLR (Fig. 4b–c). In all the nuclear loci, the Chamba population shares one of their haplotypes with the eastern populations. The exception to this is seen in the UBN1 network

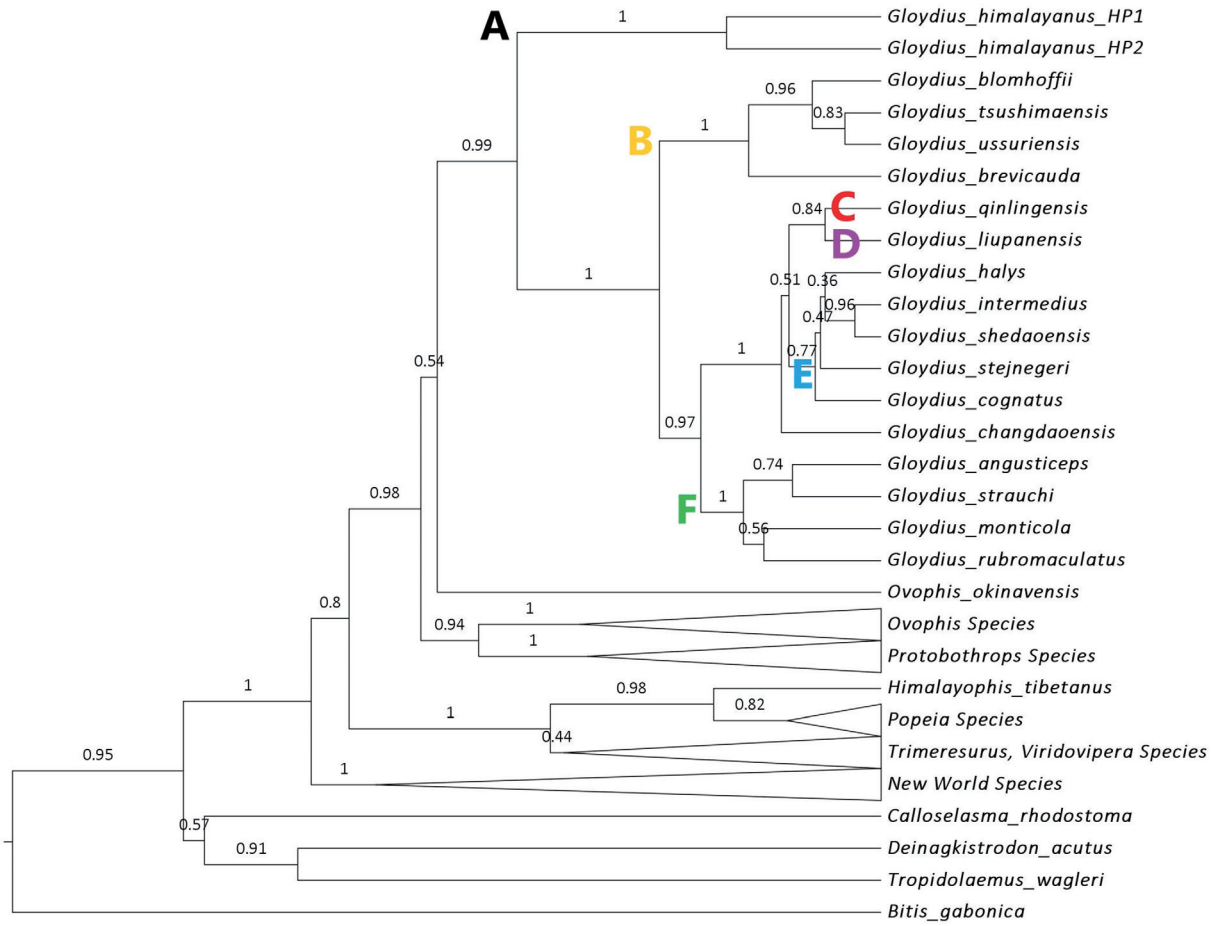

Fig. 3. Multispecies coalescent tree from *Beast. The tips indicate the assigned taxa, and branch labels are posterior probabilities. Clades A–F are as in Fig. 2. The tip labelled "Gloydius_himalayanus_HP1" corresponds to the Chamba specimens and HP2 to the samples from eastern Himachal Pradesh.

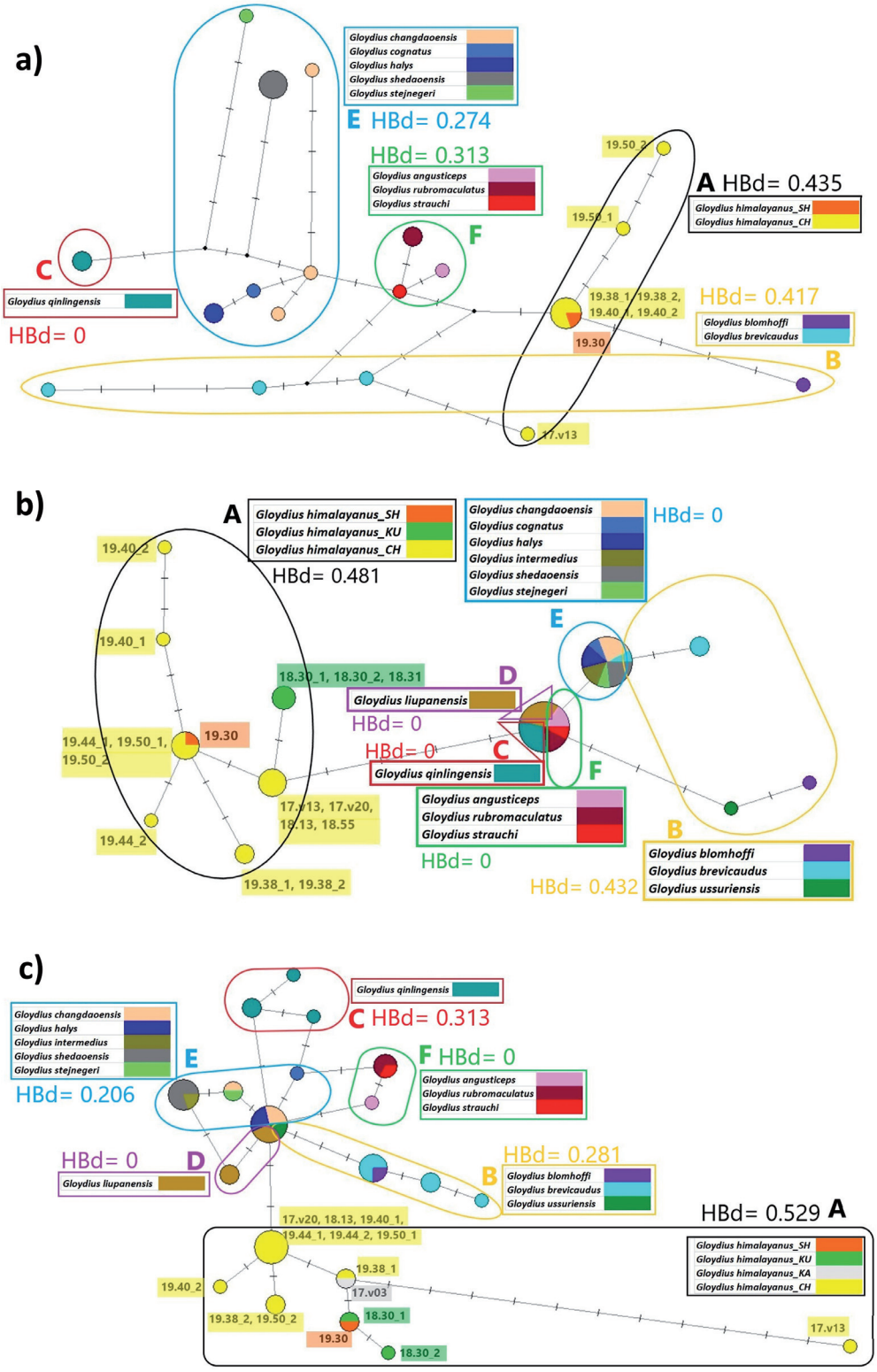

Fig. 4 (continued on next page). Median-joining haplotype networks of all nuclear genes, with clades identified in mitochondrial and multi-locus phylogenetic trees indicated by boxes labelled as a) RAG1; b) cmos; c) PRLR; d) UBN1; e) NT3. The haplotype network branch diversity (HBd) for each clade is indicated in a box in each gene network.

(Fig. 4d), where the Chamba population has a set of haplotypes that are entirely distinct from the rest of the specimens of the species. Sharing of haplotypes among species in the rest of the genus is a common occurrence in almost all loci. In cmos, a single haplotype is shared among species belonging to Clades C, D and F; the single haplotype found in all Clade E species is also shared with *G. brevicauda* from Clade B. In the NT3 network (Fig. 4e), *G. strauchi* (Clade F) and *G. brevicauda* (Clade B) share a haplotype, while two haplotypes of *G. changdaoensis* are found in an entirely separate location in the network from the rest of Clade E. In the PRLR network (Fig. 4c), one haplotype is shared among species belonging to Clades B, D and E.

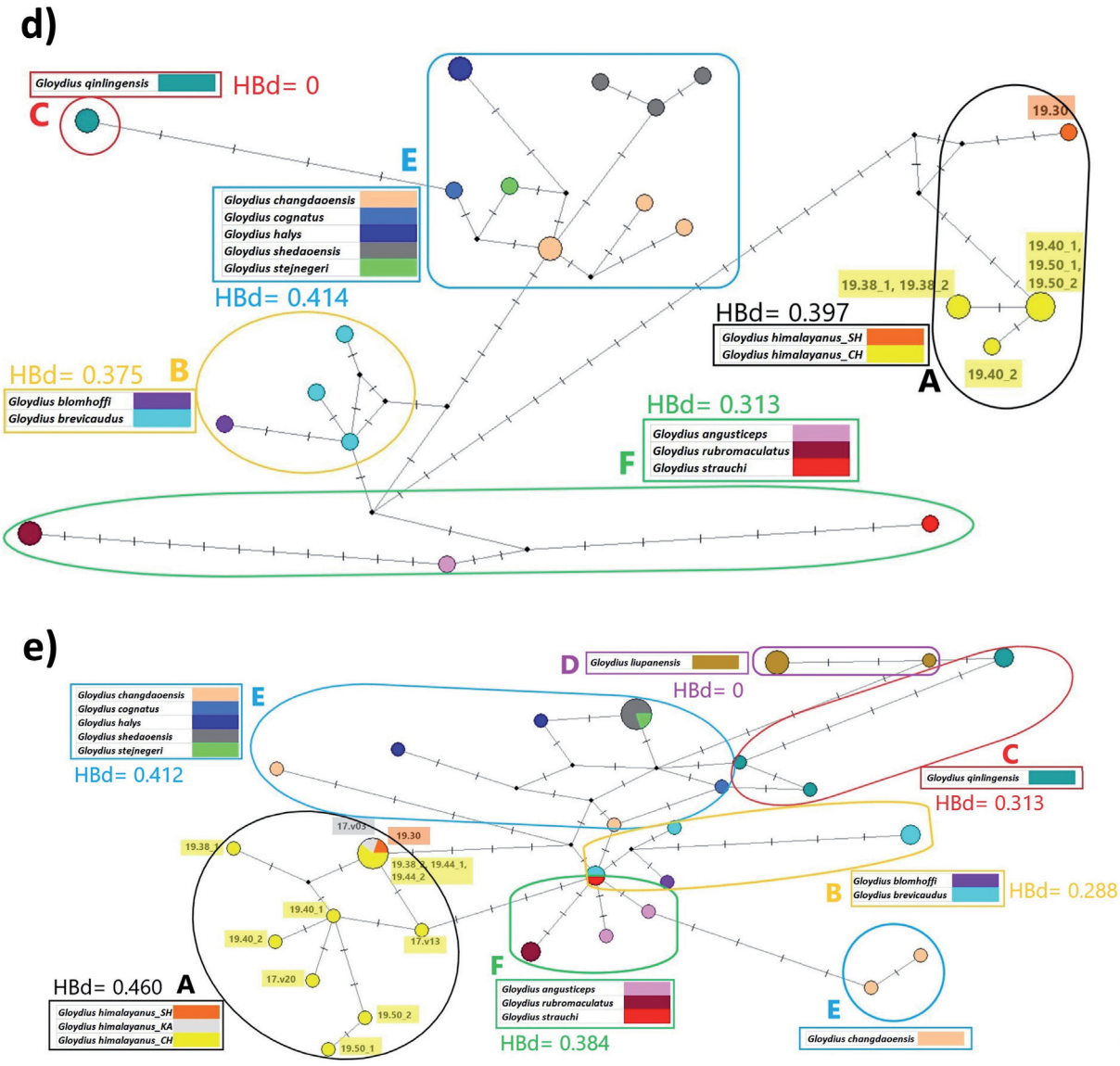

Fig. 4 (continued). Median-joining haplotype networks of all nuclear genes, with clades identified in mitochondrial and multi-locus phylogenetic trees indicated by boxes labelled as a) RAG1; b) cmos; c) PRLR; d) UBN1; e) NT3. The haplotype network branch diversity (HBd) for each clade is indicated in a box in each gene network.

Population genetics metrics

For network metrics, many of the clades had HBd as 0, due to either the presence of only a single haplotype or having two haplotypes, where there can only be a single branch (Fig. 4). The *G. himalayanus* clade (clade A) had the highest value of HBd compared to the other clades in all the genes apart from UBN1, where clade E had a higher value of 0.414 compared to 0.397 (Fig. 4). The difference between the HBd value of clade A and the HBd value of the clade with the closest value is less than 0.05 in all genes (RAG1 = 0.019; cmos = 0.049; NT3 = 0.047; UBN1 = 0.018) apart from PRLR, where it is 0.216.

Morphology

The only character that was found to be significantly different between males and females was 8to6DV ($F = 1.742$, df 1, 22, $P = 0.008$). This was excluded from further analysis so that all specimens could be pooled to maximise sample size. The small sample sizes in the initial groups based on location made it impossible to carry out Levene's test for homogeneity of variances and, for most characters, robust tests of equality of means. For the initial investigation, therefore, characters showing significant differences between localities in the ANOVA were accepted. These were: Latgular ($P = 0.043$), Suplab ($P = 0.031$), Sublab ($P = 0.02$), Supoc ($P = 0.001$), Fusedup ($P = 0.001$), Eye ($P = 0.014$), Intnas ($P = 0.011$), Stripe ($P = 0.001$), Strtemp ($P < 0.001$), Spot100 ($P = 0.002$), 23to21VS ($P = 0.024$), 19to17VS ($P = 0.004$), 14to12SC ($P = 0.001$), 14to12DV ($P = 0.028$), 12to10SC ($P < 0.001$), 8to6SC ($P = 0.015$). The only mensural character which showed a marginally significant difference among localities in ANCOVA was Whead2 (Lhead as covariate, $P = 0.057$). However, when adjusted against Lhead using the equation Whead2+(20.6-Lhead)*0.778 where 20.6 is the grand mean for Lhead, and 0.778 is the regression coefficient of Whead2 against Lhead, the among-locality ANOVA was not significant. Thus, no mensural characters were included in subsequent analyses.

Principal component analysis was carried out using a) all the selected characters (n = 18), b) without scale reduction characters, Stripe or Spot100 (n = 22), and c) also without Supoc, Fusedup and Strtemp in order to include the maximum available specimens (n = 29). The analysis including the most characters showed Chamba specimens from Churah forming a discrete group, while specimens from the west of this (Eastern Pakistan, USNM 51491 with a vague location "Kashmir") were very similar to other specimens from Srinagar in the Valley of Kashmir (Fig. 5a). Specimens from eastern localities in Himachal Pradesh (Kullu Valley, GHNP, Shimla, with the latter two being identified as East HP in Figure 5) formed a discrete group. A specimen with no location information other than "the Himalayas" was somewhat intermediate between eastern and western specimens. However, specimens from Kargil, Chilas (both in Kashmir), Dalhousie (southern Chamba district) and Garhwal (Uttarakhand) were not represented.

In the analysis in which characters that are missing in a large number of specimens (mostly scale reduction characters) were removed, the specimens from Kargil are now included and are similar to those from other western locations (Fig. 5b). While the separation between eastern and western groups on PC2 is reduced, the specimen from "the Himalayas" now groups clearly with the eastern locations, while the specimen from "Kashmir" groups with other western locations. The distinction between the Churah specimens and all others is maintained. In the final PCA, including the most specimens but the fewest characters (Fig. 5c), the distinction between groups is unsurprisingly much less pronounced but still present. This is the only analysis that includes Dalhousie specimens, and interestingly they appear very diverse, with at least one specimen (from Kalatop Wildlife Sanctuary, somewhat to the north of Dalhousie) grouping with Churah specimens, while others appear to be more similar to both eastern and western groups. Given this apparent diversity, Dalhousie specimens were left ungrouped in the subsequent analyses.

Screening of among-locality differences using ANOVA (and robust alternatives) and ANCOVA was then repeated using the new groups (eastern, western, Churah) for all characters. By and large the same set of characters were selected, but a few changed from significant to insignificant, or vice versa. A few marginally insignificant characters (at the 5% level) were retained for multivariate analysis. The final set of characters used were: Latgular, Supoc, Sublab, Stripe, Strtemp, Spot75, Spot100, 25to23VS, 23to21VS, 19to17VS, 19to17DV, 14to12SC, 14to12DV, 12to10SC, 10to8DV, 8to6SC, and 6to4SC. However, Spot75 and Spot100 are highly correlated (r = 0.814), so Spot75 was removed, as Spot100 is easier to score.

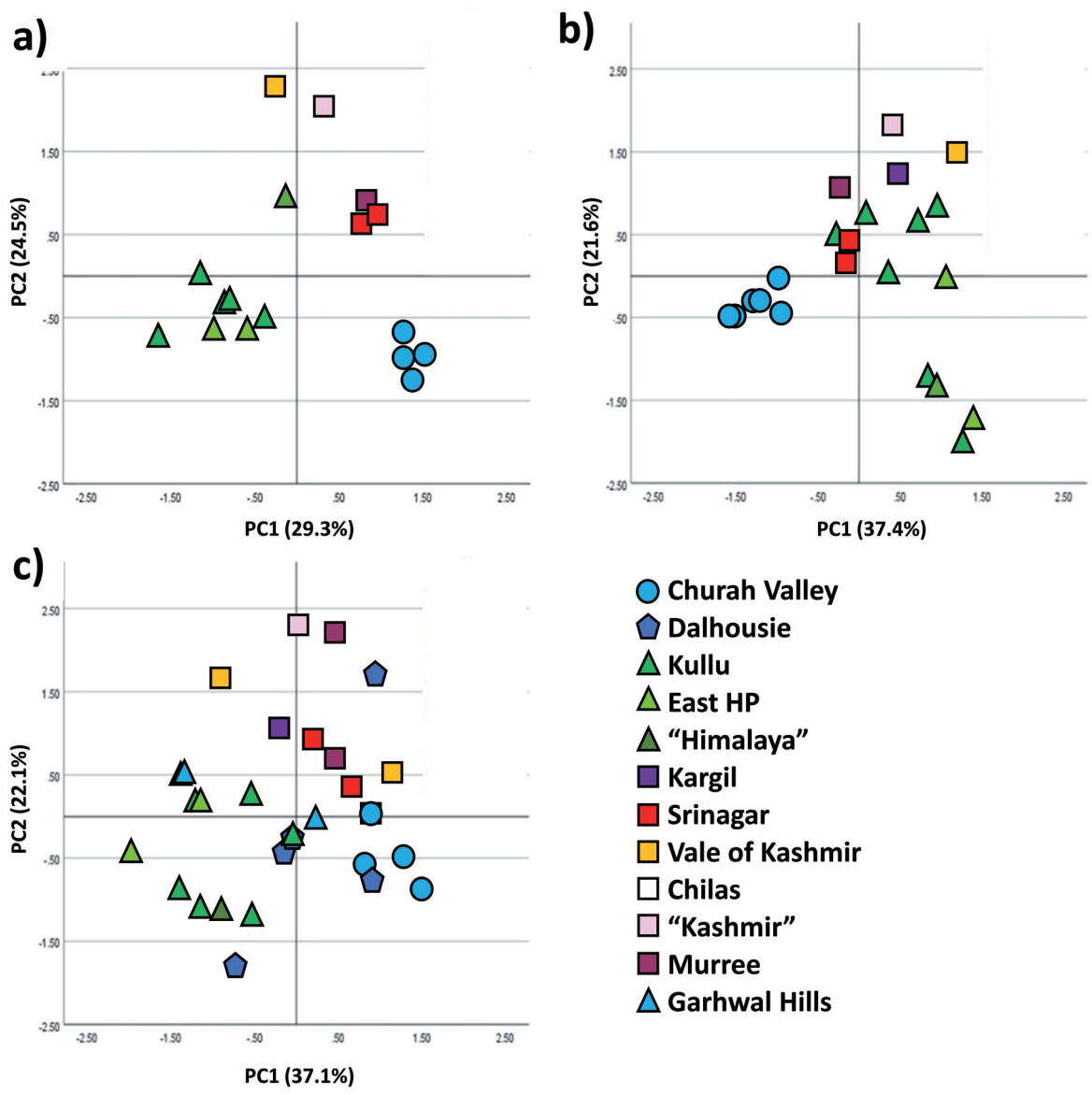

Fig. 5. Principal components analysis of *Gloydius himalayanus* (Günther, 1864) morphological data. Different analyses represent different combinations of characters and specimens as described in the text, a trade-off required by the presence of missing data. **a**. More characters, fewer specimens (n = 18). **b**. Intermediate number of characters and specimens (n = 22). **c**. More specimens, fewer characters (n = 31). This analysis does not require *a priori* grouping; hence the symbols are added for interpretation only.

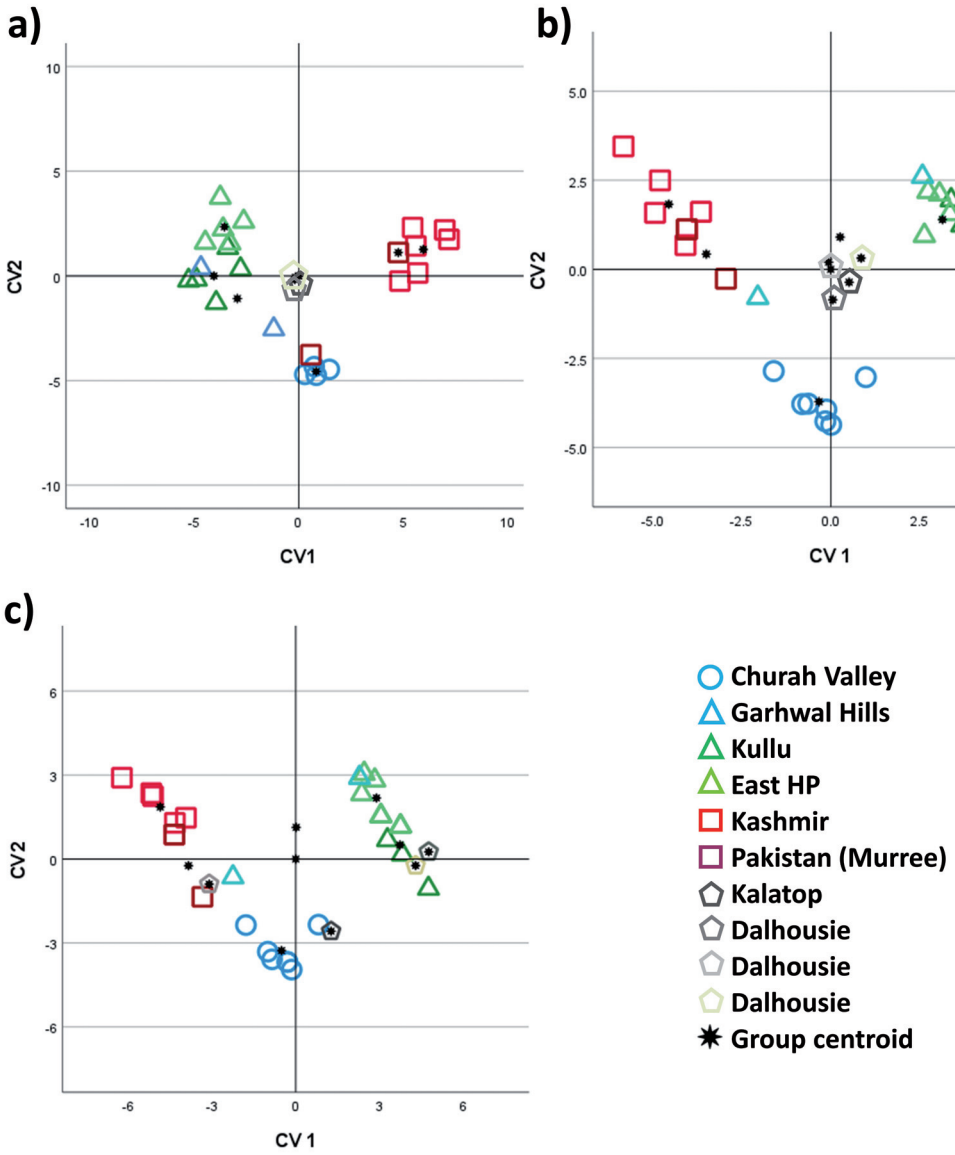

Fig. 6. Canonical Variate analysis of *Gloydius himalayanus* (Günther, 1864) morphological data. Different analyses represent different combinations of characters and specimens as described in the text, a trade-off required by the presence of missing data. **a**. More characters, fewer specimens (n = 24): the main discriminating characters on CV1 are Supoc (with lower counts at more positive values), 14to12SC, 12to10SC and 8to6SC (occurring more posteriorly at more positive values) and on CV2 are Latgular, Strtemp, Supoc (with higher counts at more positive values). **b**. Intermediate number of characters and specimens (n = 27): the main discriminating characters on CV1 is Supoc (with higher counts at more positive values), and on CV2 are Latgular, Stripe, Supoc (with higher counts at more positive values) and Stripe and Sublab (with higher counts at more negative values). **c**. More specimens, fewer characters (n = 31): the main discriminating characters on CV1 is Supoc (with higher counts at more positive values), and on CV2 are Latgular and Strtemp (with higher counts at more positive values). This analysis requires *a priori* groups to be defined; however, Dalhousie/Kalatop specimens were plotted onto axes extracted using all other groups. In these analyses, CV1 and CV2 summarise 82, 85, and 95% of the variation present, respectively, with CV1 representing ca 60% in all cases.

Canonical variate analysis (CVA) was performed with variables transformed, as described above for PCA, using a stepwise procedure (where at each step the variable that maximises the Mahalanobis distance between the two closest groups is added) with six groups: Churah, Kullu Valley, Eastern HP, Garhwal, Kashmir, and Pakistan. Dalhousie specimens were plotted on the resulting axes but were not included in the extraction. In the first analysis, with all the characters named above included, 24 specimens were included (Fig. 6a). The general grouping seen in PCA of three clusters (Churah, eastern and western) was maintained, with the five Dalhousie specimens grouping closely and falling within the eastern cluster. However, unexpectedly, one of the Pakistan specimens (BNHS 2515 from Ghora Galli) was positioned very close to the Churah cluster. Characters were then iteratively eliminated to include more specimens, as described above. When n = 26, the Ghora Galli specimen was in the expected position compared to the rest of the western specimens. It therefore seems likely that some of the scale reduction characters were incorrectly scored. The most specimens (n = 31) were included when all scale reduction characters, Spot100 and Stripe were excluded (Fig. 6c) and resulted in less distinction between clusters, with Dalhousie specimens in particular becoming more spread out, with one grouping with the western cluster (along with a specimen from Garhwal) and one with the Churah specimens. The discriminant analysis between Churah and all other specimens maintained the significance of Latgular, Sublab, Strtemp and Stripe in distinguishing between these groups, with Churah having a higher Latgular count and Strtemp proportion, and a lower Sublab count and Stripe length.

Finally, a discriminant function analysis between the Chamba Valley and remaining specimens found that three characters alone, Latgular, Sublab and Strtemp, which are relatively easy to measure, can discriminate these groups with 100% success (including in cross-validation tests where each case is classified by the functions derived from all other cases other than that case). However, it should be borne in mind that the small sample size and the lack of specimens from the eastern part of the range in this study means that these discriminating characteristics will require re-examination once more data is obtained.

In view of the distinctiveness of the Chamba specimens in both genetic and morphological analyses, we hereby describe this population as a new species.

Taxonomy

Class Reptilia Laurenti, 1768
Order Squamata Oppel, 1811
Family Viperidae Gray, 1825
Genus *Gloydius* Hoge & Romano-Hoge, 1981

Gloydius chambensis sp. nov.
urn:lsid:zoobank.org:act:3FC261AB-C7DD-4E7F-92F6-0FBC5607B46C
Figs 7–9

Halys himalayanus Günther, 1864: 393, pl. 24 fig. a (only specimens from Chamba District).

Ancistrodon himalayanus – Boulenger 1896: 424, fig. 125. — Smith 1943: 495–496, fig. 157.
Agkistrodon himalayanus – Gloyd & Conant 1990: 255–264, pl. 14, 31, 38, 52 figs 20–23.
Agkistrodon himalayana – Underwood 1999: 3–8.
Gloydius himalayanus – McDiarmid *et al.* 1999: 305. — Gumprecht *et al.* 2004: 20–21, figs i–iii (p. 64), i–iii (p. 65). — Wallach *et al.* 2014: 310.

Diagnosis

Gloydius chambensis sp. nov. can be identified by the number of gular scales in contact with the infralabial scales (4–5, mean 4.17), number of sublabial scales (9–10, mean 9.57) and the proportion of the first temporal scale covered by the postocular stripe (covering less than a quarter of the temporal scale).

Differential diagnosis

Gloydius chambensis sp. nov. can be distinguished from its sister species, *G. himalayanus*, by the lower number of gular scales in contact with the infralabial scales (4–5, mean 4.17, compared to 5–6, mean 5.67, in *G. himalayanus*), a higher number of sublabial scales, r (9–10, mean 9.57, compared to 6–9, mean 7.97, in *G. himalayanus*) and a lower proportion of the first temporal scale covered by the postocular stripe (covering less than a quarter of the temporal scale, compared to more than a quarter in *G. himalayanus*).

Both *Gloydius chambensis* sp. nov. and *Gloydius himalayanus* can be distinguished from all other congeneric species by a very distinct or sharp canthus rostralis (Gloyd & Conant 1990), from the *Gloydius halys* complex by having 21 mid-body dorsal rows (vs 22 or 23 rows) (Shi *et al.* 2018), from *G. rubromaculatus*, *G. strauchi* and *G. huangi* Wang, Ren, Dong, Jiang, Shi, Siler, & Che, 2019 by having a pointed snout and triangular head (vs a blunt snout and rounded head) (Shi *et al.* 2017, 2018; Wang *et al.* 2019) and from *G. angusticeps* and *G. monticola* by having a matte dorsal texture (vs a glassy texture with a metallic lustre) (Shi *et al.* 2018; Wang *et al.* 2019).

Etymology

The specific epithet '*chambensis*' means 'from Chamba' in reference to the species being distributed in Chamba District. The suggested common name is the 'Chamba Pitviper'.

Type material

Holotype

INDIA • ♂ adult; Himachal Pradesh, Chamba District, Bhanjraru; 10 Jul. 2018; 32.83909° N, 76.14932° E; alt. 1738 m; Sourish Kuttalam, Vishal Santra, John Benjamin Owens, Vipin Dhiman, Anita Malhotra, Nilanjan Mukherjee, Stuart Graham and Anatoli Togridou leg; found dead on the road; GenBank: OP422588, OP450868, OP407966, OP518269; Voucher Specimen R259 (DNA reference number 18.13); HARC R259 (collection of the High Altitude Research Centre, Solan, Himachal Pradesh).

Holotype description

The holotype HARC R259 is an adult male with a snout-vent length of 34 cm and a tail length of 8.6 cm (total length = 42.6 cm). The width of the head is 13.84 mm and the length of the head is 19.21 mm. The diameter of the eye is 2.78 mm. The head is distinctly triangular and the canthus rostralis is sharp and conspicuous.

Scalation

The holotype has one scale between the nasal scale and the loreal heat-sensing pit, one scale between the loreal pit and the preocular scale, and two postocular scales. The supraocular scale has a completely smooth outer edge. The border of the internasal scales and prefrontal scales is distinctly convex or curved (vs a concave or flat border in eastern populations in Himachal Pradesh). There are seven supralabial scales with the third supralabial scale in contact with the lower postocular scale. The penultimate supralabial scale is fused with the last temporal scale. The specimen has 10 infralabial scales. It has four gular scales in contact with the infralabial scales (not including from the enlarged chin shields). The dorsal scales are in 25:21:17 rows, with heavy keeling on all the dorsal scales. The number of ventral scales is 164 and the number of subcaudal scales is 42.

Coloration in life (Fig. 7)

Paired distinct dark-coloured stripes start from the posterior head scales and extend down the neck and dorsolateral surface as far as the 20th ventral scale. The postocular stripe is a thin, dark brown stripe that begins from the rear edge of the eye and continues onto the two temporal scales, impinging slightly on

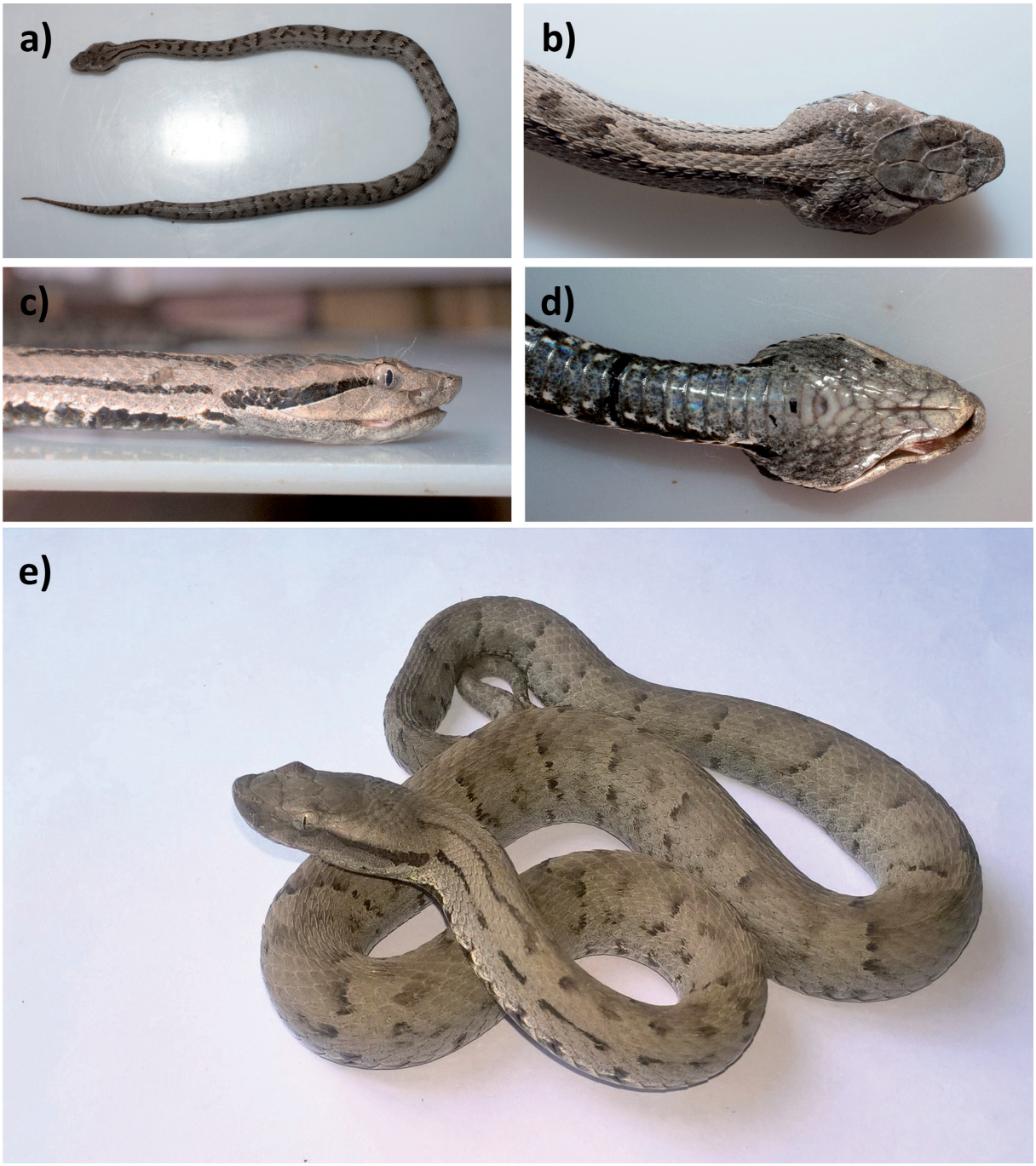

Fig. 7. a–d. *Gloydius chambensis* sp. nov., holotype, ♂ (Specimen Number 18.13; Churah Valley, HARC R359). **a**. Whole body **b–d**. Close-up of the head in dorsal (b), lateral (c) and ventral (d) views. **d**. The first and 10th ventrals have been marked with black marker to assist with counting scales. **e**. A whole body view of specimen 17.v20 from Bhanjraru, Chamba. Photos provided by J.B. Owens and V. Santra.

the last supralabial scale. The lower edge of the ocular stripe is bordered by a white line. The longer of the two ocular stripes ends in line with the 4th ventral scale. A total of 24 crossbands on the dorsal surface of the body. These are a dull mud-brown colour, with some having a darker inner border. There are also blotches all along the lateral sides of the body that are broken extensions of the crossbands. The ventral scales are glossy, with many scales having blotches with white edges on the ends of the scale, similar to those on the lateral surface. The background dorsal coloration is a dull mud-brown colour with a matte texture. The posterior half of the tail is lighter in colour.

Variation

Whilst the holotype shares most characters with the rest of the specimens of Chamba, there are some differences. In the scale counts, the holotype has a higher number of ventral scales (164 vs 158–161). In coloration, it differs in the number of crossbands found on the body (24 vs 29–39). The first two scale reductions (25 to 23 and 23 to 21) occur closer to the head (the reduction from 25 to 23 scales occurs at 14.94% vs 5%–8%; 23 to 21 scales at 21.34% vs 8%–11%).

Taxonomic remarks

All specimens that were examined and diagnosed to be *Gloydius chambensis* sp. nov. were specimens from the field study site. Apart from the deposited holotype, none of the other field specimens were

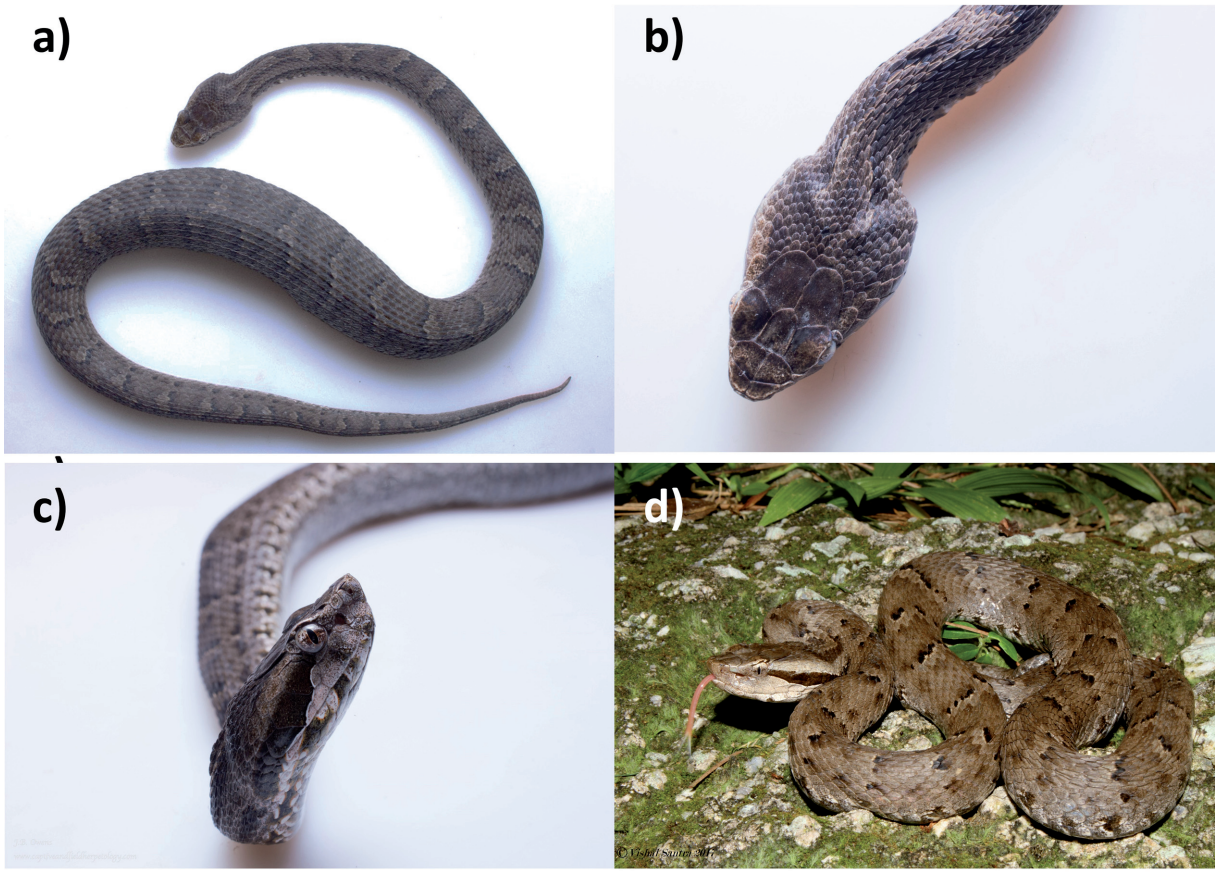

Fig. 8. *Gloydius himalayanus* (Günther, 1864). **a–c**. Male specimen (Great Himalayan National Park, Himachal Pradesh, India; Specimen Number: 18.30). **a**. Whole body. **b–c**. Close-up views of the dorsal (b) and lateral (c) head. **d**. Specimen 17.v03 (Palampur, Kangra), whole body in-situ. Photos provided by J.B. Owens and V. Santra.

found dead. Our collecting permits did not allow us to ethically euthanise live individuals for this study. Hence, no paratype has been designated.

Distribution and habitat

Gloydius chambensis sp. nov. is distributed across the Chamba and associated valleys, which has an elevational range from 400 m to 5500 m. The major river system of the valley is the Ravi River (Ghosh & Chhibber 1984). The valley is isolated by two ranges, the Pir Panjal Range to the north and northwest and the Dhauladhar Range to the south and southeast (Fig. 1). The specimens were found in habitat primarily consisting of alpine scrub and pine forests, with a ground layer of thick pine needle litter (Fig. 9). The habitat was interspersed with occasional boulders and rock faces. Almost all the specimens were found close to rural households, and anecdotal interactions with the local villagers indicate that this is the venomous snake that is most commonly seen in the region and that causes the most bites to people in the valley (Fig. 10). Some studies have noted that bites can result in pain, swelling, bruising, and bleeding (Khan & Tasnim 1986; Raina *et al.* 2014).

Discussion

In our multi-locus study, phylogenetic analysis of a concatenated mitochondrial dataset strongly supported the Chamba population, heretofore considered *Gloydius himalayanus*, as a distinct species. The median-joining networks of nuclear genes (apart from RAG1) agreed with mitochondrial phylogeny in showing a large genetic distance between the *G. himalayanus* clade and the remaining species of *Gloydius*, but did not distinctly separate the Chamba population from the rest of the eastern Himachal

Fig. 9. The habitat of *Gloydius chambensis* sp. nov. in Chamba District, Himachal Pradesh, India (elevation = 1700 m). Photo by V. Santra.

Fig. 10. Examples of bites from *Gloydius chambensis* sp. nov. **a**. Female victim bitten on the little toe of her left foot, while walking through long grass to collect drinking water, with visible swelling. **b–c**. Elderly woman, bitten on the ring finger of her right hand while cutting long grass for cattle fodder, with swelling, localized pain, and tenderness immediately after the bite. After 24 hours, there were signs of infection at the bite site with reduced swelling. The substances on the leg of the first victim and the white substance on the hand of the second victim were applied by a local faith healer.

Pradesh specimens, as seen in the analysis of the mitochondrial dataset, with the exception of UBN1. In most cases, although there were several private haplotypes, at least one haplotype was shared between the putative new species and other populations. However, this could represent ancestral haplotypes that have been retained within the populations. Most nuclear loci showed such haplotype sharing between other well-established species of *Gloydius*, some of which belong to relatively distant mitochondrial clades (e.g., *G. brevicauda* and *G. strauchi* for NT3; Clades B, D and E for PRLR). This could indicate a low level of genetic variation at those loci, which suggests that there may be incomplete lineage sorting of ancestral polymorphisms or low levels of sequence evolution (Wan *et al.* 2004). Higher values of HBd in general indicate that the population has a higher genetic diversity as well as haplotypes that are well connected with the potential presence of rare variants (Garcia *et al.* 2021). The HBd value for clade A, the clade that contains the new species as well as its sister species *G. himalayanus*, is the highest in all genes, apart from UBN1, where it has the second highest value. The difference between clade A and the other clades that contain multiple recognised species is very small, in all apart from PRLR, indicating that the diversity and connectivity shown between *G. himalayanus* and *G. chambensis* sp. nov. is similar to that seen in other multi-species clades. Such findings further support the species-level separation between the new species and *G. himalayanus*. In addition, the multi-species coalescent analysis conducted in this study was congruent with the findings of the mitochondrial data when it comes to the distinction of the Chamba population from remaining *Gloydius himalayanus* specimens sampled in Himachal Pradesh, thus indicating that the mitochondrial gene trees are not confounded by effects such as genetic linkage, maternal inheritance, and incomplete lineage sorting (Nesi *et al.* 2011; Fonseca & Lohmann 2020; Li *et al.* 2020), which is why it is problematic to rely solely on mtDNA when making polygenetic inferences (Ballard & Whitlock 2004; Edwards 2009; Galtier *et al.* 2009; Toews & Brelsford 2012; Grechko 2013; Folt *et al.* 2019; Marshall *et al.* 2021). Here, we have followed the recommended practice in phylogenetic analysis of combining both mitochondrial and nuclear DNA loci in a coalescent model (Edwards *et al.* 2016) in order to reliably infer evolutionary histories and resolve species limits. Increased sampling to evaluate current or past gene flow in the contact zones between two closely related species (Mebert 2008; Hillis 2019) is desirable but not always achievable in the case of cryptic snake species. Here, we analysed morphological data (which is represented by polygenic characters) from a larger sample than represented in the genetic analysis and found additional support for the elevation of the Chamba population.

The Dhauladhar Range, varying in elevation from 300 m to 5000 m a.s.l., borders the Chamba Valley, Churah Valley and other deep valleys of the region (Fig. 1), while the Pir Panjal Range running along the north-western border of the valley (Thiede *et al.* 2017) provides a further physical barrier that could account for the geographic isolation of *G. chambensis* sp. nov.

The exact distribution of the new species in the Chamba district requires further survey effort, as it may extend as far south as the Kalatop Wildlife Sanctuary. The specimens labelled "Dalhousie", which appear to have disparate affinities, may originate from other locations; such labelling practices were not unusual during the British Raj when these specimens were collected. A more extensive study, including specimens from further east in Uttarakhand, Nepal, and Bhutan, may also reveal additional diagnostic characters for *G. chambensis* sp. nov. For example, in our data, *G. chambensis* shares some characters with specimens from Kashmir and Pakistan. Among the specimens examined here, all specimens from Chamba, Kashmir and Pakistan had a smooth-edged supraocular while those from eastern locations possessed a supraocular with a distinct notch on the rear edge. However, Gloyd & Conant (1990) include a diagram of a specimen from Nathia Gali, Pakistan, very close to the specimen examined here from Murree, which possesses a notched supraocular, so this may be an artefact of sample size.

Our findings also further support the basal position of *G. himalayanus* within the rest of *Gloydius* (Shi *et al.* 2021). Xu *et al.* (2012) conducted divergence estimate studies on *Gloydius* and suggested that the

group originated during the mid-Miocene (~15 Ma) with speciation within the group beginning in the late Miocene (~9.8 Ma). At this time, the Qinghai-Xizang plateau had begun to uplift, and the rate of uplift increased in the late Miocene (Copeland *et al.* 1987). The Himalayan orogen also changed from a North–South extension to a North–South contraction during the mid-Miocene (Wang *et al.* 2013). A study of the oxygen isotopic composition of the modern water of southern Tibet and the Himalayas indicated that the present-day hypsometry of this region was achieved by the late-Miocene, about 10 Ma (Rowley *et al.* 2001). Studies have also indicated that it was sometime between the mid- and late-Miocene that the Dhauladhar Range was formed due to the uplifting activity of the Main Boundary Thrust (Adlakha *et al.* 2013; Thiede *et al.* 2017).With such geological changes occurring, it is possible the populations of *Gloydius* on the southern slopes of the Himalayan peaks were isolated by physical barriers from the majority of the current species of *Gloydius*, accounting for the large genetic separation and basal position of *G. himalayanus*.

In conclusion, the phylogenetic analysis of *Gloydius himalayanus* using various inference methods on both mitochondrial and nuclear data indicate that there is a cryptic species present within *G. himalayanus*, as currently recognised. Combined with the morphological analysis, this investigation confirms the discovery of *Gloydius chambensis* sp. nov. as the second species of *Gloydius* distributed on the Indian subcontinent.

Acknowledgements

The Himachal Pradesh Forest Department granted permission to carry out the sample collection under permit number FEE-FB-F(10)-3/2017. The funding for this work was provided by the European Union Seventh Framework Programme (under grant agreement number PIRSES-GA-2013-612131) to the BITES consortium in 2017, the Second Tibetan Plateau Scientific Expedition and Research Program (grant no. 2019QZKK0705 to Tao Deng), and a small grant from The Rufford Foundation to Vishal Santra (Offer Letter: 25313-1) in 2018. We owe a huge debt of gratitude to Vipin Dhiman, our logistical manager and local guide in Himachal Pradesh, without whom none of this would have been possible. We thank Molla Talhauddin Ahmed, Anweshan Patra, Sankha Suvra Nandy, Richard Southworth, Jasmine Torrez, Luke O'Sullivan, Maya Master, Teddy Gilbert, and James McConnell for volunteering their assistance with the fieldwork. We are grateful to Priyanka Swamy, Princia D'Souza, Vidisha Kulkarni, and Somdipta Sen for helping with the lab work at the Centre for Ecological Sciences, IISc. KS thanks the DBT-IISc Partnership Programme for support. Since the first draft of this paper was prepared, one of the co-authors, Melvin Selvan, sadly has passed away. He was a dedicated and gifted herpetologist and conservationist, and a beloved friend to many of us. We dedicate this paper to his memory.

References

Adlakha V., Patel R.C., Lal N., Mehta Y.P., Jain A.K. & Kumar A. 2013. Tectonics and climate interplay: exhumation patterns of the Dhauladhar Range, northwest Himalaya. *Current Science* 114 (11): 1551–1559.

Alencar L.R., Quental T.B., Grazziotin F.G., Alfaro M.L., Martins M., Venzon M. & Zaher H. 2016. Diversification in vipers: phylogenetic relationships, time of divergence and shifts in speciation rates. *Molecular Phylogenetics & Evolution* 105: 50–62. https://doi.org/10.1016/j.ympev.2016.07.029

Ballard J.W.O. & Whitlock M.C. 2004. The incomplete natural history of mitochondria. *Molecular Ecology* 13 (4): 729–744. https://doi.org/10.1046/j.1365-294X.2003.02063.x

Bandelt H.J., Forster P. & Röhl A. 1999. Median-joining networks for inferring intraspecific phylogenies. *Molecular Biology & Evolution* 16 (1): 37–48. https://doi.org/10.1093/oxfordjournals.molbev.a026036

Barido-Sottani J., Bošková V., Plessis L.D., Kühnert D., Magnus C., Mitov V., Müller N.F., Pečerska J., Rasmussen D.A., Zhang C. & Drummond A.J. 2018. Taming the BEAST — A community teaching material resource for BEAST 2. *Systematic Biology* 67 (1): 170–174. https://doi.org/10.1093/sysbio/syx060

Bouckaert R. & Xie D. 2017. BEAST2-Dev/substmodels: standard nucleotide substitution models v1.0.1. https://doi.org/10.5281/zenodo.995740

Boulenger A. 1896. *Catalogue of Snakes in the British Museum.* Vol. III. Taylor & Francis, London. https://doi.org/10.5962/bhl.title.8316

Brown M.B. & Forsythe A.B. 1974. Robust tests for the equality of variances. *Journal of the American Statistical Association* 69 (346): 364–367. https://doi.org/10.1080/01621459.1974.10482955

Chaudhuri A., Mukherjee S., Chowdhury S. & Purkayastha J. 2018. *Gloydius himalayanus* (Himalayan pitviper). *Herpetological Review* 49 (3): 505.

Chettri B., Bhupathy S. & Acharya B.K. 2011. An overview of the herpetofauna of Sikkim with emphasis on the elevational distribution pattern and threats and conservation issues. *In*: Arrawatia M.L.& Tambe S. (eds) *Biodiversity of Sikkim – Exploring and Conserving a Global Hotspot*: 233–254. Information & Public Relations Department, Government of Sikkim, Gangtok.

Copeland P., Harrison T.M., Kidd W.E.A., Ronghua X. & Yuquan Z. 1987. Rapid early Miocene acceleration of uplift in the Gangdese Belt, Xizang (southern Tibet), and its bearing on accommodation mechanisms of the India-Asia collision. *Earth & Planetary Science Letters* 86 (2–4): 240–252. https://doi.org/10.1016/0012-821X(87)90224-X

Darriba D., Taboada G.L., Doallo R. & Posada D. 2012. jModelTest 2: more models, new heuristics and parallel computing. *Nature Methods* 9 (8): 772. https://doi.org/10.1038/nmeth.2109

Edgar R.C. 2004. MUSCLE: a multiple sequence alignment method with reduced time and space complexity. *BMC Bioinformatics* 5 (1): 1–19. https://doi.org/10.1186/1471-2105-5-113

Edwards S.V. 2009. Is a new and general theory of molecular systematics emerging? *Evolution* 63 (1): 1–19. https://doi.org/10.1111/j.1558-5646.2008.00549.x

Edwards S.V., Xi Z., Janke A., Faircloth B.C., McCormack J.E., Glenn T.C., Zhong B., Wu S., Lemmon E.M., Lemmon A.R. & Leaché A.D. 2016. Implementing and testing the multispecies coalescent model: a valuable paradigm for phylogenomics. *Molecular Phylogenetics & Evolution* 94: 447–462. https://doi.org/10.1016/j.ympev.2015.10.027

Folt B., Bauder J., Spear S., Stevenson D., Hoffman M., Oaks J.R., Wood Jr P.L., Jenkins C., Steen D.A. & Guyer C. 2019. Taxonomic and conservation implications of population genetic admixture, mito-nuclear discordance, and male-biased dispersal of a large endangered snake, *Drymarchon couperi*. *PLoS One* 14 (3): e0214439. https://doi.org/10.1371/journal.pone.0214439

Fonseca L.H.M. & Lohmann L.G. 2020. Exploring the potential of nuclear and mitochondrial sequencing data generated through genome-skimming for plant phylogenetics: a case study from a clade of neotropical lianas. *Journal of Systematics & Evolution* 58 (1): 18–32. https://doi.org/10.1111/jse.12533

Galtier N., Nabholz B., Glémin S. & Hurst G.D.D. 2009. Mitochondrial DNA as a marker of molecular diversity: a reappraisal. *Molecular Ecology* 18 (22): 4541–4550. https://doi.org/10.1111/j.1365-294X.2009.04380.x

Garcia E., Wright D., Gatins R., Roberts M.B., Pinheiro H.T., Salas E., Chen J.Y., Winnikoff J.R. & Bernardi G. 2021. Haplotype network branch diversity, a new metric combining genetic and topological diversity to compare the complexity of haplotype networks. *PLoS One* 16 (6): e0251878. https://doi.org/10.1371/journal.pone.0251878

Ghosh D.K. & Chhibber I.B. 1984. Aid of photointerpretation in the identification of geomorphic and geologic features around Chamba-Dharamsala area, Himachal Pradesh. *Journal of the Indian Society of Photo-Interpretation & Remote Sensing* 12 (1): 55–64.

Gloyd H.K. & Conant R. 1990. Snakes of the *Agkistrodon* complex: a monographic review. *Contributions to Herpetology* 6. Society for the Study of Amphibians & Reptiles, St. Louis.

Grechko V.V. 2013. The problems of molecular phylogenetics with the example of squamate reptiles: mitochondrial DNA markers. *Molecular Biology* 47 (1): 55–74. https://doi.org/10.1134/S0026893313010056

Guindon S. & Gascuel O. 2003. A simple, fast, and accurate algorithm to estimate large phylogenies by maximum likelihood. *Systematic Biology* 52 (5): 696–704. https://doi.org/10.1080/10635150390235520

Gumprecht A., Tillack F., Orlov N., Captain A. & Ryabov S. 2004. *Asian Pitvipers*. Geitje Books, Berlin.

Günther A.C.L.G. 1864. *The Reptiles of British India*. Hardwicke [Ray Society], London. https://doi.org/10.5962/bhl.title.5012

Hasegawa M., Kishino H. & Yano, T.A. 1985. Dating of the human-ape splitting by a molecular clock of mitochondrial DNA. *Journal of Molecular Evolution* 22 (2): 160–174. https://doi.org/10.1007/BF02101694

Heath T.A. 2015. Divergence time estimation using BEAST v2.2.0. Tutorial written for workshop on applied phylogenetics and molecular evolution, Bodega Bay, California. Available from http://treethinkers.org/tutorials/divergence-time-estimation-using-beast/ [accessed 8 Nov. 2022].

Heled J. & Drummond A.J. 2010. Bayesian inference of species trees from multilocus data. *Molecular Biology & Evolution* 27 (3): 570–580. https://doi.org/10.1093/molbev/msp274

Hillis D.M. 2019. Species delimitation in herpetology. *Journal of Herpetology* 53 (1): 3–12. https://doi.org/10.1670/18-123

Hoge A.R. & Romano-Hoge S.A.R.W.D.L. 1981. Poisonous snakes of the world. Part 1. Check list of the pitvipers, Viperoidea, Viperidae, Crotalinae. *Memórias do Instituto Butantan* 42: 179–310.

Kalyaanamoorthy S., Minh B.Q., Wong T.K., Von Haeseler A. & Jermiin L.S. 2017. ModelFinder: fast model selection for accurate phylogenetic estimates. *Nature Methods* 14 (6): 587–589. https://doi.org/10.1038/nmeth.4285

Khan M.S. & Tasnim R. 1986. Notes on the Himalayan pitviper, *Agkistrodon himalayanus* (Günther). *Litteratura Serpentium, Ser. English edition* 6: 46–55.

Kimura M. 1980. A simple method for estimating evolutionary rates of base substitutions through comparative studies of nucleotide sequences. *Journal of Molecular Evolution* 16 (2): 111–120. https://doi.org/10.1007/BF01731581

Kimura M. 1981. Estimation of evolutionary distances between homologous nucleotide sequences. *Proceedings of the National Academy of Sciences of the United States of America* 78 (1): 454–458. https://doi.org/10.1073/pnas.78.1.454

Koirala B.K., Gurung D.B., Lhendup P. & Phuntsho S. 2016. Species diversity and spatial distribution of snakes in Jigme Dorji National Park and adjoining areas, western Bhutan. *Journal of Threatened Taxa* 8 (12): 9461–9466. https://doi.org/10.11609/jott.2617.8.12.9461-9466

Kumar S., Stecher G. & Tamura K. 2016. MEGA7: Molecular Evolutionary Genetics Analysis version 7.0 for bigger datasets. *Molecular Biology & Evolution* 33 (7): 1870–1874. https://doi.org/10.1093/molbev/msw054

Lanfear R., Frandsen P.B., Wright A.M., Senfeld T. & Calcott B. 2017. PartitionFinder 2: new methods for selecting partitioned models of evolution for molecular and morphological phylogenetic analyses. *Molecular Biology & Evolution* 34 (3): 772–773. https://doi.org/10.1093/molbev/msw260

Lartillot N. & Philippe H. 2004. A Bayesian mixture model for across-site heterogeneities in the amino-acid replacement process. *Molecular Biology & Evolution* 21 (6): 1095–1109. https://doi.org/10.1093/molbev/msh112

Levene H. 1961. Robust tests for equality of variances. *In*: Olkin I. (ed.) *Contributions to Probability and Statistics*. *Essays in Honor of Harold Hotelling*: 279–292. Stanford University Press, Palo Alto, CA.

Li J.N., Liang D., Wang Y.Y., Guo P., Huang S. & Zhang P. 2020. A large-scale systematic framework of Chinese snakes based on a unified multilocus marker system. *Molecular Phylogenetics & Evolution* 148: e106807. https://doi.org/10.1016/j.ympev.2020.106807

Malhotra A., Creer S., Pook C.E. & Thorpe R.S. 2010. Inclusion of nuclear intron sequence data helps to identify the Asian sister group of New World pitvipers. *Molecular Phylogenetics & Evolution* 54 (1): 172–178. https://doi.org/10.1016/j.ympev.2009.09.007

Manhas A. 2020. Observations of Himalayan pitvipers, *Gloydius himalayanus* (Günther, 1864), in the Doda District, Jammu and Kashmir, India. *Reptiles & Amphibians* 27 (3): 476–478. https://doi.org/10.17161/randa.v27i3

Marshall T.L., Chambers E.A., Matz M.V. & Hillis D.M. 2021. How mitonuclear discordance and geographic variation have confounded species boundaries in a widely studied snake. *Molecular Phylogenetics & Evolution* 162: e107194. https://doi.org/10.1016/j.ympev.2021.107194

McDiarmid R.W., Campbell J.A. & Touré T. 1999. *Snake Species of the World: A Taxonomic and Geographic Reference*. Vol. 1. Herpetologists' League, Washington, D.C.

Mebert K. 2008. Good species despite massive hybridization: genetic research on the contact zone between the watersnakes *Nerodia sipedon* and *N. fasciata* in the Carolinas, USA. *Molecular Ecology* 17 (8): 1918–1929. https://doi.org/10.1111/j.1365-294X.2008.03725.x

Minh B.Q., Nguyen M.A.T. & von Haeseler A. 2013. Ultrafast approximation for phylogenetic bootstrap. *Molecular Biology & Evolution* 30 (5): 1188–1195. https://doi.org/10.1093/molbev/mst024

Nesi N., Nakoune E., Cruaud C. & Hassanin A. 2011. DNA barcoding of African fruit bats (Mammalia, Pteropodidae). The mitochondrial genome does not provide a reliable discrimination between *Epomophorus gambianus* and *Micropteropus pusillus*. *Comptes Rendus Biologies* 334 (7): 544–554. https://doi.org/10.1016/j.crvi.2011.05.003

Nguyen L.T., Schmidt H.A., Von Haeseler A. & Minh B.Q. 2015. IQ-TREE: a fast and effective stochastic algorithm for estimating maximum-likelihood phylogenies. *Molecular Biology & Evolution* 32 (1): 268–274. https://doi.org/10.1093/molbev/msu300

Orlov N.L. & Barabanov A.V. 2000. About type localities for some species of the genus *Gloydius* Hoge et Romano-Hoge, 1981 (Crotalinae: Viperidae: Serpentes). *Russian Journal of Herpetology* 7 (2): 159–160.

Posada D. 2003. Using MODELTEST and PAUP* to select a model of nucleotide substitution. *Current Protocols in Bioinformatics* 1: 6-5. https://doi.org/10.1002/0471250953.bi0605s00

Qiagen 2020. *DNeasy Blood & Tissue Handbook*. Available from https://www.qiagen.com/ [accessed 27 Oct. 2022].

R Core Team 2020. R: a language and environment for statistical computing. R Foundation for Statistical Computing, Vienna, Austria. Available from https://www.R-project.org/ [accessed 27 Oct. 2022].

Raina S., Raina S., Kaul R., Chander V. & Jaryal A. 2014. Snakebite profile from a medical college in rural setting in the hills of Himachal Pradesh, India. *Indian Journal of Critical Care Medicine* 18 (3): 134–138. https://doi.org/10.4103/0972-5229.128702

Ronquist F., Teslenko M., Van Der Mark P., Ayres D.L., Darling A., Höhna S., Larget B., Liu L., Suchard M.A. & Huelsenbeck J.P. 2012. MrBayes 3.2: efficient Bayesian phylogenetic inference and model choice across a large model space. *Systematic Biology* 61 (3): 539–542. https://doi.org/10.1093/sysbio/sys029

Rowley D.B., Pierrehumbert R.T. & Currie B.S. 2001. A new approach to stable isotope-based paleoaltimetry: implications for paleoaltimetry and paleohypsometry of the High Himalaya since the Late Miocene. *Earth & Planetary Science Letters* 188 (1–2): 253–268. https://doi.org/10.1016/S0012-821X(01)00324-7

Rozas J., Ferrer-Mata A., Sánchez-DelBarrio J.C., Guirao-Rico S., Librado P., Ramos-Onsins S.E. & Sánchez-Gracia A. 2017. DnaSP 6: DNA sequence polymorphism analysis of large data sets. *Molecular Biology & Evolution* 34 (12): 3299–3302. https://doi.org/10.1093/molbev/msx248

Shi J., Wang G., Fang Y., Ding L., Huang S., Hou M., Liu J. & Li P. 2017. A new moth-preying alpine pitviper species from Qinghai-Tibetan Plateau (Viperidae, Crotalinae). *Amphibia-Reptilia* 38 (4): 517–532. https://doi.org/10.1163/15685381-00003134

Shi J., Yang D., Zhang W., Peng L., Orlov N.L., Jiang F., Ding L., Hou M., Huang X., Huang S. & Li P. 2018. A new species of the *Gloydius strauchi* complex (Crotalinae: Viperidae: Serpentes) from Qinghai, Sichuan, and Gansu, China. *Russian Journal of Herpetology* 25 (2): 126–138. https://doi.org/10.30906/1026-2296-2018-25-2-126-138

Shi J.S., Liu J.C., Giri R., Owens J.B., Santra V., Kuttalam S., Selvan M., Guo K.J. & Malhotra A. 2021. Molecular phylogenetic analysis of the genus *Gloydius* (Squamata, Viperidae, Crotalinae), with description of two new alpine species from Qinghai-Tibet Plateau, China. *ZooKeys* 1061: 87–108. https://doi.org/10.3897/zookeys.1061.70420

Smith M.A. 1943. *The Fauna of British India, Ceylon and Burma, Including the Whole of the Indo-Chinese Sub-region*. *Reptilia & Amphibia. Vol. III. Serpentes*. Taylor and Francis, London.

Tamura K. & Nei M. 1993. Estimation of the number of nucleotide substitutions in the control region of mitochondrial DNA in humans and chimpanzees. *Molecular Biology & Evolution* 10 (3): 512–526. https://doi.org/10.1093/oxfordjournals.molbev.a040023

Tavaré S. 1986. Some probabilistic and statistical problems in the analysis of DNA sequences. *Lectures on Mathematics in the Life Sciences* 17 (2): 57–86.

Thiede R., Robert X., Stübner K., Dey S. & Faruhn J. 2017. Sustained out-of-sequence shortening along a tectonically active segment of the Main Boundary thrust: the Dhauladhar Range in the northwestern Himalaya. *Lithosphere* 9 (5): 715–725. https://doi.org/10.1130/L630E.1

Toews D.P. & Brelsford A. 2012. The biogeography of mitochondrial and nuclear discordance in animals. *Molecular Ecology* 21 (16): 3907–3930. https://doi.org/10.1111/j.1365-294X.2012.05664.x

Underwood G. 1999. Morphological evidence on the affinities of vipers. *In*: Joger U. (ed.) *Phylogeny and Systematics of the Viperidae*. *Kaupia, Darmstädter Beiträge zur Naturgeschichte* 8: 3–8.

Wagner P., Tiutenko A., Mazepa G., Borkin L.J. & Simonov E. 2016. Alai! Alai! – a new species of the *Gloydius halys* (Pallas, 1776) complex (Viperidae, Crotalinae), including a brief review of the complex. *Amphibia-Reptilia* 37 (1): 15–31. https://doi.org/10.1163/15685381-00003026

Wall F. 1910. A popular treatise on the common Indian snakes. Part XIII. *Journal of the Bombay Natural History Society* 20: 65–79.

Wallach V., Williams K.L. & Boundy J. 2014. *Snakes of the World: A Catalogue of Living and Extinct Species*. Taylor and Francis, CRC Press, Boca Raton, FL, USA.

Wan Q.H., Wu H., Fujihara T. & Fang S.G. 2004. Which genetic marker for which conservation genetics issue? *Electrophoresis* 25 (14): 2165–2176. https://doi.org/10.1002/elps.200305922

Wang K., Ren J., Dong W., Jiang K., Shi J., Siler C.D. & Che J. 2019. A new species of Plateau Pit Viper (Reptilia: Serpentes: *Gloydius*) from the Upper Lancang (= Mekong) Valley in the Hengduan Mountain Region, Tibet, China. *Journal of Herpetology* 53 (3): 224–236. https://doi.org/10.1670/18-126

Wang X., Zhang J., Liu J., Yan S. & Wang J. 2013. Middle-Miocene transformation of tectonic regime in the Himalayan orogen. *Chinese Science Bulletin* 58 (1): 108–117. https://doi.org/10.1007/s11434-012-5414-6

Warren D.L., Geneva A.J. & Lanfear R. 2017. RWTY (R We There Yet): an R package for examining convergence of Bayesian phylogenetic analyses. *Molecular Biology & Evolution* 34 (4): 1016–1020. https://doi.org/10.1093/molbev/msw279

Whitaker R. & Captain A. 2004. *Snakes of India.* Draco Books, Chengalpattu, Tamil Nadu, India.

Xu Y., Liu Q., Myers E.A., Wang L., Huang S., He Y., Peng P. & Guo P. 2012. Molecular phylogeny of the genus *Gloydius* (Serpentes: Crotalinae). *Asian Herpetological Research* 3: 127–132. https://doi.org/10.3724/SP.J.1245.2012.00127

Manuscript received: 28 April 2022
Manuscript accepted: 13 September 2022
Published on: 13 December 2022
Topic editor: Tony Robillard
Section editor: Aurélien Miralles
Desk editor: Pepe Fernández

Supplementary file

Supp. file 1. Additional information. https://doi.org/10.5852/ejt.2022.852.2003.8181

Table S1. PCR primers used in this study along with their sequences.

Table S2. The PCR programs used for each gene in this study. The range given for the annealing temperatures indicates that some variation was required to produce usable PCR products.

Table S3. List of Accession Number for the species of *Gloydius* Hoge & Romano-Hoge, 1981 used in this study. The accession numbers for the sequences produced for this study have been highlighted in yellow. The country and region code are as per the ISO-3166 standard published by the International Organization of Standardisation (https://www.iso.org/iso-3166-country-codes.html).

Fig. S1. Parameter Trace Plots- RWTY will produce trace and density plots of each column statistic in the trace file. For example, in this study, a parameter trace and density plot were created for the log likelihood of each cold chain (LnL). Such plots are useful to help tune further analysis (e.g., burn-in). The title of each plot shows the Effective Sample Size (ESS). In general, all the parameters should have an ESS>200, which was achieved in this study.

Fig. S2. Tree topology plots are like the parameter plots. They reveal where the MCMC was sampling from a stationary distribution of chains or whether moving between different modes. They also show how well-mixed the chains are with respect to tree topologies. Well-mixed chains will show the trace jumping rapidly between values.

Fig. S3. The plots show the split frequencies of clades in the chain either as the frequency calculated from cumulative samples in the chain at various points in the analysis or as the frequency within the sliding window. By default, they show the 20 clades with the highest standard deviation od split frequencies within each sample. In analysis that is mixing well, the frequencies in the cumulative plot should level off and the frequencies in the sliding window to move around a lot. If the frequencies in the cumulative window are not levelled off, it may mean the chain had to run longer.

Fig. S4. The plots demonstrate the movement of the chains in two dimensional representations of treespace. The space is created using all the chains together, hence, the treespaces of different chains are comparable. The treespace plots for all the chains will looks similar if the chains are sampling similar tree topologies.

Fig. S5. The Average Standard Deviation of Split Frequencies (ASDSF) of clades that appear in any of the chains, are calculated from cumulative samples in the chain at various points in the analysis. The solid line shows the ASDSF and the ribbons the 75%, 95% and 100% quantiles of the Standard Deviation of the Split Frequencies (SDSF) across the clades. A lower ASDSF indicates that the chains are more in agreement on split frequencies. The y-axis is plotted on a log10 scale. In general, the SDSF is expected to get lower as the chains progress.

Fig. S6. Split Frequency scatterplot matrix shows the how much agreement is there between regions of treespace the chains have sampled. For each comparison, the cumulative final frequency of each clade in a chain is plotted against the same on another chain. The correlation (Pearson's R) and ASDSF for each pair of chains is also shown. A satisfactory agreement will have the R-value between 0.9 and 1.0, and the ASDSF value will be lesser than 0.01.

Fig. S7. The ASDSF dendogram shows the similarity of split frequencies between chains. The more similar ones are grouped together. This plot helps indicate which chains are sampling similar region of the treespace.

Fig. S8. Bayesian Tree: Branch labels indicate the posterior probabilties (%). In this and subsequent figures, each clade is labelled and designated in a particular colour. These clades are, A. *Gloydius himalayanus* (Black); B. *G. blomhoffi*, *G. brevicaudus*, *G. ussuriensis* (Yellow); C. *G. qinlingensis* (Red); D. *G. liupanensis* (Purple); E. *G. halys*, *G. intermedius*, *G. changdaoensis*, *G. cognatus*, *G. stejnegeri*, *G. shedaoensis* (Blue); F. *G. angusticeps*, *G. strauchi*, *G. monticola*, *G. rubromaculatus* (Green).

Appendix

Appendix 1. A list of all other, apart from the holotype of *Gloydius chambensis* sp. nov., specimens used in the morphological analysis along with their depositories. Abbreviations: BNHS = Bombay Natural History Society; BNHM = British Natural History Museum; MCZ = Museum of Comparative Zoology, Harvard; NMW = Natural History Museum, Vienna (Naturhistorisches Museum Wien); USNM = Smithsonian National Museum of Natural History; ZSI Solan = High Altitude Research Centre, Zoological Survey of India, Solan, Himachal Pradesh.

Gloydius himalayanus (Günther, 1864)

INDIA • 2 ♂♂, 2 ♀♀; Dalhousie; BNHS 2507, BNHS 2508, BNHS 2513, BNHS 2514 • 3 ♂♂, 2 ♀♀, 1 spec. sex unknown; Kullu; BNHS 2505, MCZ Herp-R3138, MCZ Herp-R3139(A), MCZ Herp-R3139(B), MCZ Herp-R3140 • 1 ♀; Garwhal, UP; alt. 1700 ft; BNHS 2520 • 1 ♂; Guptkashi, Garwhaal Himalayas; BNHS 2885 • 1 ♀; Chilas, Kashmir; BNHS 2519 • 3 ♀♀; Srinagar, Kashmir; NWM 17079.20, NWM 17079.10, USNM 20884 • 1 ♀; Palawar, Kashmir; USNM 48471 • 1 ♂; Kashmir; USNM 51491 • 1 ♀; Kotgarh, Himachal Pradesh; NMW15134.1 • 1 ♂; Himalayas; BNHM 1872.4.17.363 • 1 ♀; Kalatop Work Station, Khajjiar, Himachal Pradesh; ZSI Solan • 1 ♀; Dumas, Bairagarh, Himachal Pradesh; examined in field (18.54) • 2 ♀♀; Khushnagri, Himchal Pradesh; examined in field (18.55, 19.38) • 1 ♀; Tharvai, Himachal Pradesh; examined in field (19.40) • 1 ♂; Bairagarh, Himachal Pradesh; examined in field (19.44) • 1 spec. sex unknown; Manju, Himachal Pradesh; examined in field (19.50) • 2 ♀♀; Sainj, Himachal Pradesh; examined in field (18.30, 18.31) • 1 ♀; Dhevu, near Sarahan, Himachal Pradesh; examined in field (19.30).

PAKISTAN • 1 ♂; Murree, Rawalpindi District; NMW 17078 • 1 ♂; Ghora Galli, Punjab; BNHS 2515..